4WWM 105-1

4TH WEATHER WING MANUAL

AD648073

Weather

# FORECASTING SOLAR ACTIVITY AND GEOPHYSICAL RESPONSES

30 December 1966



DEPARTMENT OF THE AIR FORCE

Distribution of this document is unlimited.

Hq ADC Field Printing Plant
Ent AFB, Colorado

# FORECASTING SOLAR ACTIVITY

# AND

# GEOPHYSICAL RESPONSES

30 December 1966

Solar Forecast Facility
Headquarters, 4th Weather Wing
Ent Air Force Base, Colorado

BLANK PAGE

# F O R E W O R D

As Air Force interest in space environment increases, progress continues in the prediction of solar and geophysical parameters. Experience and new knowledge gained since the original publication of this manual in April 1966 are largely responsible for the three-fold increase in its size. Verification programs have enabled us to identify the most successful techniques for standardization as well as the false premises to be discarded and the areas of difficulty to be analyzed more systematically. Standardization of observing equipment and reporting procedures has helped to increase the effectiveness of our verification programs and the objectivity of our forecasting techniques. However, in spite of all this progress, the increased recognition of space environmental effects on military operations has left us with more unsolved problems than we had before.

This second edition of the solar and geophysical forecasters' handbook is the product of the combined efforts of all officers and non-commissioned officers assigned to the Solar Forecast Center and the Detachment headquarters. Compiling, editing, and publishing have been the responsibility of Capt Allan C. Ramsay, Scientific Services Officer for the Solar Forecast Facility. Further revisions are planned at frequent intervals over the next several years. Studies under way at the Solar Forecast Center and research work in progress at the Air Force Cambridge Research Laboratories are already producing results to be included in the next revision. These efforts are receiving additional emphasis, and continuing progress is anticipated.

Charles K. Anderson

CHARLES K. ANDERSON, Colonel, USAF
Director, Solar Forecast Facility

THIS IS A BLANK PAGE

4WW MANUAL
NO. 105-1

HEADQUARTERS 4TH WEATHER WING (MAC)
Ent Air Force Base, Colorado 80912
30 December 1966

Weather

# FORECASTING SOLAR ACTIVITY AND GEOPHYSICAL RESPONSES

PURPOSE: To discuss the philosophy and the techniques involved in producing probability forecasts for the occurrence of solar flares and proton events, forecasts of 10-cm solar radio flux, and forecasts of the geomagnetic index $A_p$ and to describe the principal parameters and relationships to be considered and evaluated in making these forecasts.

CONTENTS



This Manual supersedes 4WWM 105-1 1 April 1966
OPR: 4VVC
DISTRIBUTION: X (Determined by OPR

THIS IS A BLANK PAGE

# Chapter 1

## SOLAR FLARE FORECAST

1.1 General. Prior to the augmentation of SOFNET observing and forecasting sites by AWS personnel, it was believed that a well-defined separation could be maintained between short- and long-range predictions of solar activity. Ideally, the short-range forecasts would be made at the observatories by experienced observer-forecasters using information directly available to them through white light and H-alpha instruments; these forecasts would be modified very little (if at all) before being disseminated to using agencies. Long-range forecasts would be prepared at the Solar Forecast Center; various (unspecified) theoretical, empirical, or statistical relationships would be used with apparent trends to extrapolate current reports of solar activity into the future. Unfortunately, this forecasting scheme has proved to be impractical; it has become necessary for the Solar Forecast Center to involve itself in the details of producing both short-range (24-hour) and long-range (up to five-day) flare forecasts. The procedures used to arrive at the solar flare forecasts issued by the Solar Forecast Center are discussed below.

1.2 Forecast Input:

a. Optical. Optical information available on the required near-real-time basis includes the following: sunspot type, location, area, geometrical configuration, and magnetic classification; calcium and H-alpha plage area, brightness, location, rate and intensity of fluctuation; general appearance of disk and limb in H-alpha; vortical structure; enhancement in H-alpha wings; filament activity; recent surge and flare production; enhancement of coronal red-, green-, and yellow-line emission; limb surges, and prominence characteristics.

b. Radio. Radio information includes daily flux values and burst data at about 600, 1400, 2700, 5000, and 8800 mc/s. Significant bursts at meter wavelengths (19-41 mc/s) are reported as they occur. Solar maps from the Stanford Radio Astronomy Institute (at 9.1 cm) and from the Aerospace Corp. (3.4 mm) are currently being used on a daily basis.

c. SOFNET Flare Probability Forecasts. In addition to the parameters which are routinely observed and reported to the SFC, the observer-forecaster at an observing site is able to detect more detailed structures and rapid changes in solar active regions which to a large extent are averaged out in the data received by the SFC. Plain language descriptions and the OL flare forecasts are the basic inputs which include these types of qualitative data; even small changes in successive OL forecasts are considered most carefully. The OL forecasts are accepted as one of the most valuable factors in the final flare forecast. (OL: Operating Location)

1.3 Philosophy of the Short-Range Flare Forecast:

a. At the time this is being written, the business of forecasting solar flares remains as much art as science. Studies now in progress hold a glimmer of hope for the introduction of a significant amount of objectivity into future flare forecasts.

b. Forecasts of Flare Probability. The present system of assigning a probability of occurrence of a major flare reflects the inability of the forecaster to issue a "YES/NO" prediction. For any given forecast, the correct percentage probability of a flare is either "zero" or "100"; it is the desire of the flare forecaster to minimize the "wrongness" of his forecast. In order to accomplish this, a forecaster will issue varying percentage probabilities which reflect different "shades" of "YES" and "NO":

| | |
|---|---|
| 0 | Positively NO |
| 10 | |
| 20 | NO |
| 30 | |
| 40 | Maybe NO |
| 50 | |
| 60 | Maybe YES |
| 70 | |
| 80 | YES |
| 90 | |
| 100 | Positively YES |

or:

Less than 5% = "If it flares, it'll be a surprise to us!"

5% to 15% = "It'll still be a surprise, but not such a big one."

20% to 35% = "We don't expect a flare, but things are getting interesting."

40% to 45% = "It really shouldn't flare, but it's getting close."

50% to 70% = "We should get a flare in the next 24 hours, but it's not a sure bet yet."

75% to 85% = "If it doesn't flare, it'll be a surprise to us!"

Above 85% = "We can't figure out why it isn't flaring right now!"

1.4 Forecaster Aids:

a. Three separate forms are used as aids to the forecaster. General descriptions follow:

b. Activity Level Designator. The first form, the Activity Level Designator (Figure 1-1), is not so objective as it may appear at first glance. The available predictors are listed on the left side; six activity levels and associated flare probabilities are arranged across the top of the chart. The values and ranges in the body of the chart are flexible and are constantly subject to revision. Because of the extreme flexibility of these values, a detailed discussion of individual assignments would serve no purpose. The majority of the values have been determined through studies of recent active regions and, while they are considered valid at this time, they most certainly will be changed as solar activity increases. The predictor values and probability ranges are updated at regular intervals through local studies prepared by personnel at the Solar Forecast Center. Although surges and subflares are listed as predictors, the precise relationship between rate of production and subsequent major flare activity has never been defined explicitly. Similarly, an example of data which are available but not even listed as predictors (because of our relative ignorance concerning the relationship of such data to subsequent flare occurrence) are the radio burst data at numerous frequencies available from a number of observatories. Hopefully, these and other data will serve as useful predictors of flare activity in the future.

c. Active Region History. The second of the attached forms (Figure 1-2) is the Active Region History chart; a record of the recent history (including plage area, spot group type and area, 9.1-cm radio flux and brightness temperature, flare production) is begun whenever the brightness temperature of a region exceeds 80,000 degrees or whenever the region produces an Importance I flare. This chart is a valuable aid in assessing activity trends and in reconciling disparities in reported values of various parameters. In small spot groups, for example, differences in observing conditions or techniques can make a difference of an order of magnitude in reported spot area; in larger spot groups and in plages, area reports from different observatories can easily differ by as much as 25 percent. The SFC forecaster is required to decide (often quite subjectively) how much relative weight is to be given to any one report when that report is at marked variance with reports

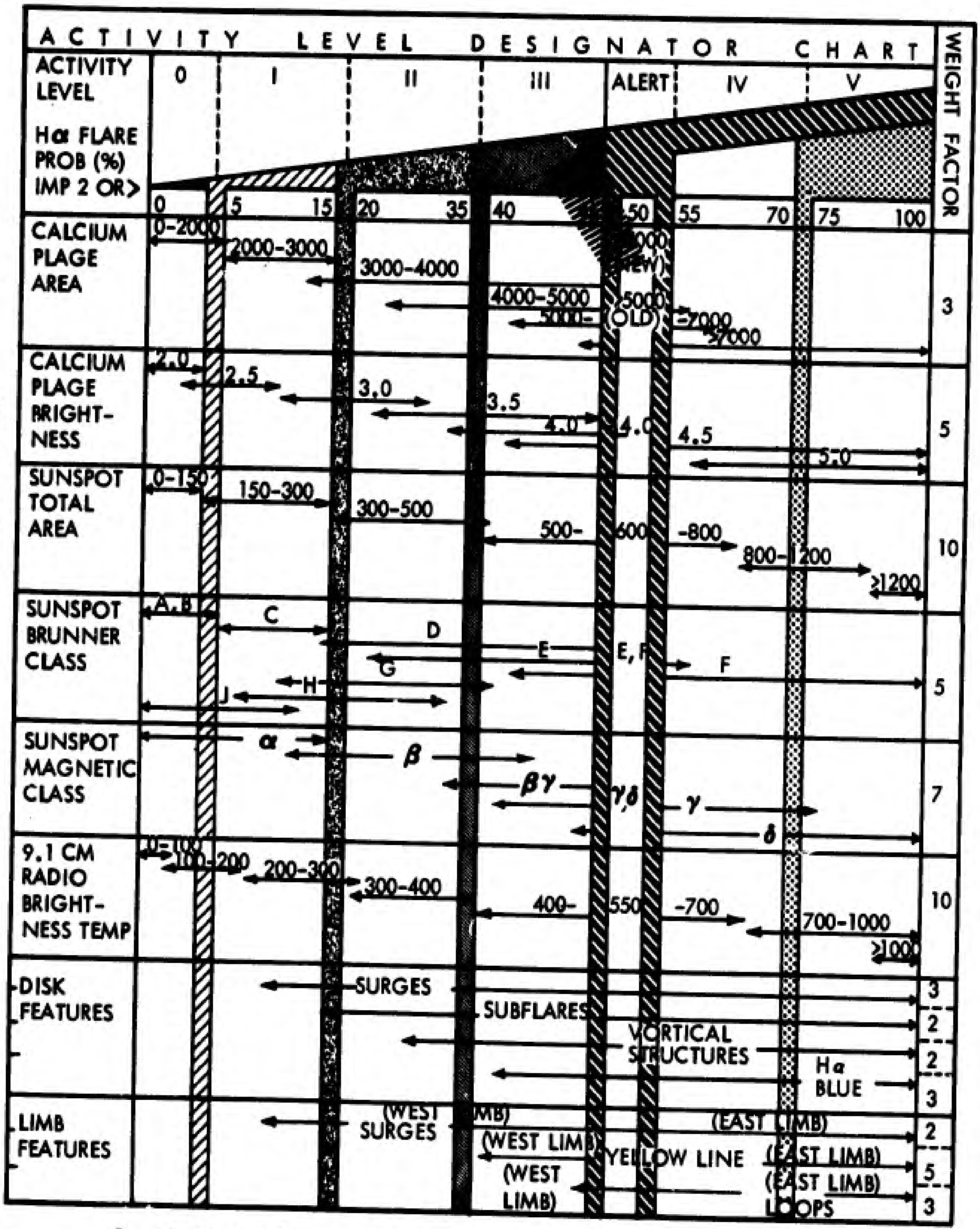


$$\overline{WP} = \frac{P_1\ wf_1 + P_2\ wf_2 + \cdots + P_n\ wf_n}{\Sigma wf_n}$$

WHERE: $\overline{WP}$ = AVERAGE WEIGHTED PROBABILITY

$P_1 \ldots P_n$ = PERCENTAGE PROBABILITY FOR INDIVIDUAL PARAMETERS

$wf_1 \ldots wf_n$ = WEIGHT FACTOR FOR INDIVIDUAL PARAMETERS (BASED ON MAXIMUM RELIABILITY OF 10)

Figure 1-1

SFC # 25

Return of SFC # (new)

Longitude 224°
Latitude +19°
CMP 19.7 Jan

Sunspot:
Sac Peak # 222
Manila # 040
Athens # 040

Ca Plages:
McMath # 131
Manila # 117

Corona:

| | Limb East | Limb West |
|---|---|---|
| Red | 1 | 1 |
| Green | 2 | 4 |
| Yellow | None | None |

Flares

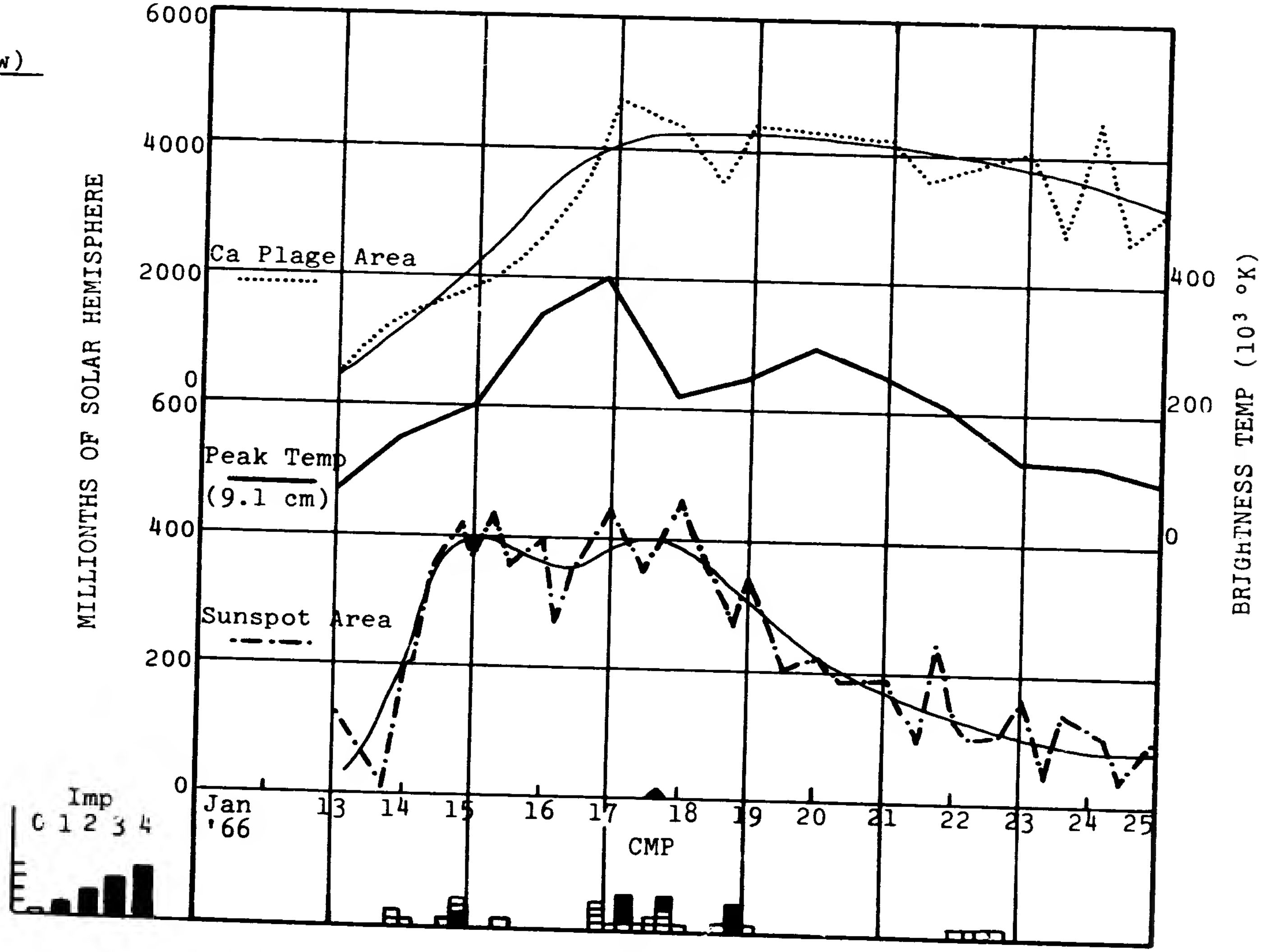


ACTIVE REGION HISTORY CHART

Figure 1-2

from other observatories and with observed trends in whatever parameter is in question.

d. Forecaster Checklist. The third form (Figure 1-3), the SFC Forecaster Checklist, is designed as a "memory-jogger" to be sure that every available predictor is considered by the forecaster. It serves as a record of the thoughts that went into the forecast and is therefore a valuable analysis tool.

1.5 Short-Range Forecast Procedure:

a. The foundation of the 24-hour flare forecast is the assessment of the flare potential of each active region on the disk (and, in some cases, the assessment of active regions which are expected to rotate over the E limb onto the visible disk).

b. Assignment of Flare Probability. Each of the following three techniques is used; differences in the resulting flare probabilities of individual active regions are reconciled before computing the final over-all flare probability.

(1) Activity-Level Concept. The first step of this forecast procedure is to assign each active region an activity level, indicated by one of the Roman numerals at the top of the Activity Level Designator chart (Figure 1-1). Activity level selection is based upon the spot group type and area, plage area and intensity, peak radio brightness temperature, etc. No single value on the chart can be considered both necessary and sufficient for the assignment of a particular activity level: a small spot group which is growing rapidly, associated with a large plage of high intensity and a moderate radio noise source, could be assigned almost any level; the forecaster must weigh each bit of information in relation to all other data in order to choose the most appropriate level. The forecaster determines current values and apparent trends of flare predictors from OL reports and from Active Region History charts (Figure 1-2). He then combines subjective information from the Checklist (Figure 1-3) with the non-quantitative entries on the Activity Level Designator chart (spot group and plage trends, plage fluctuations, coronal emission, surges, subflares, etc.) to decide on a specific flare probability within the assigned level. In marginal cases, the subjective information under consideration may serve to change the activity level assigned to an active region. Most of the non-quantitative data used to alter the flare probability of a region are "positive" indicators; that

## SOLAR FORECAST CHECKLIST

FORECAST ISSUED: ______________ VALID: __________ TO: __________

FLARE: ______________ PROTON: ______________ F10: __________

PERSISTENCE (Stable activity level): ______________

CHANGE IN OL FCST? 1: ____ 3: ____ 4: ____ 5: ____ 6: ____

CYCLIC RELATIONSHIPS:

Return of previously active region: ______________

Return of previously inactive region: ______________

Return of characteristically active longitude: ______________

Active region passing over W limb: ______________

E-LIMB ACTIVITY: Corona:

Lat ______ R: ______ G: ______ Y: ______

Lat ______ R: ______ G: ______ Y: ______

Loops and surges: ______________

Radio emission: ______________

Flares: ______________

| FLARE FCST: Region No. | | | | | |
|---|---|---|---|---|---|
| *Calcium plage (area/intensity) | | | | | |
| *H alpha plage (area/intensity) | | | | | |
| Number of spots | | | | | |
| *Spot area (umbral/penumbral) | | | | | |
| *Spot Brunner class | | | | | |
| *Spot magnetic class | | | | | |
| *Radio emission temperature | | | | | |
| *Region fine structure | | | | | |
| ADF Fluctuating plage | | | | | |
| Active Longitude? | | | | | |
| Expected activity (+, 0, -)(past/fcst) | | | | | |
| *Weighted mean activity level | | | | | |
| P. E. FCST (in addition to above) | | | | | |
| Quadrant | | | | | |
| Plage rotation no. | | | | | |
| FLUX FCST: (in addition to above) | | | | | |
| Center-limb variation | | | | | |
| Region development (+, 0, -)(past/fcst) | | | | | |
| $A_p$ FCST: 27-day persistence | | | | | |
| Modified 27-day persistence | | | | | |
| PCA expected | | | | | |
| PCA in progress | | | | | |
| Disturbance expected | | | | | |
| Disturbance in progress | | | | | |

REMARKS:

FORECASTER:

4WW Form Apr 66 0-15 (REVISED) (4WWSF)

Figure 1-3

is, the presence of a positive indicator would tend to increase the forecast flare probability, while the lack of such an indicator would decrease the forecast flare probability. Some of these indicators are listed on the Activity Level Designator chart under "Limb Features" and "Disk Features"; others, not listed, include plage fluctuation and the rate of surge and subflare production. The ranges of uncertainties in relating a precise flare probability to a given value of a predictor are indicated by the lengths of the arrows assigned to predictor values on the chart. The specific flare probability of an active region within one of these ranges may be indicated by the growth rate of the region, as follows:

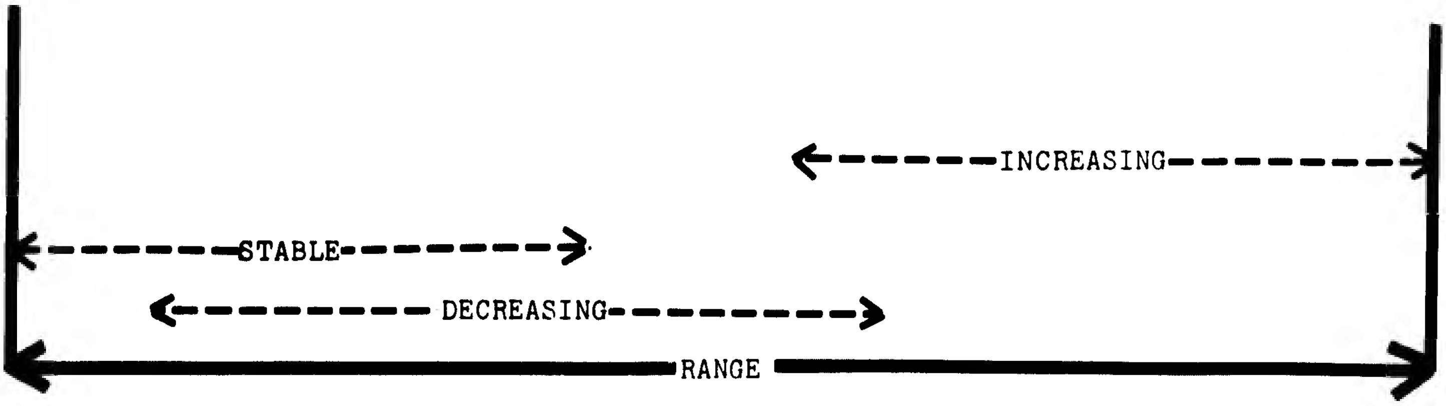


The flare probability is assigned, very subjectively, by considering the relationships that exist among all the available data, including not only the specific values of parameters reported, but also the descriptive summaries of disk and limb activity, and perhaps most important, the estimates of current solar activity and observable trends in activity indicated by the OL's in their individual 24-hour forecasts.

(2) <u>Weighted Flare Probability Concept</u>. With this technique, the flare probability of a solar active region is determined by considering each predictor independently. The forecaster enters each predictor row on the Activity Level Designator Chart (where data are available), extracts the appropriate flare probability for that predictor, multiplies each probability by its weighting factor, adds the products, and divides by the sum of the weighting factors used to arrive at the forecast. Specific flare probabilities within each range are assigned subjectively as in (1), above.

For example:

| Predictor | Predictor Value | Flare Probability | Factor | Weighted Flare Probability |
|---|---|---|---|---|
| Ca Area | 5200 | 50 | 3 | 150 |
| Ca Brightness | 3.5 | 45 | 5 | 225 |
| Spot Area | 600 | 50 | 10 | 500 |
| Brunner Class | E | 50 | 5 | 250 |
| Magnetic Class | γ | 60 | 7 | 420 |
| Radio Temp. | 720 | 80 | 10 | 800 |
| Disk Features | Small Surges | 30 | 3 | 90 |
| Limb Features | n/a | - | - | - |
| | | | 43 | 2435 |

2435/43 = 56.6%, the flare probability for this active region.

(3) Objective Technique. The first of a series of studies of solar activity designed for incorporation into a completely objective flare forecast procedure was published in April 1966 [Enger, et al., 1966]. Flare probabilities for each solar active region are computed using forecast tables based on the relationship between flare occurrence and both the size of the associated spot group and its rate of growth or dissipation. The six-hour probabilities derived from the tables are extended to cover a 24-hour period and are then compared with probabilities derived in (1) and (2), above.

c. Computation of Final 24-hour Flare Probability: Once a flare probability, $P_i$, has been assigned to each of the N regions on the disk, the total flare probability, $P_t$, is computed by

$$P_t = 1 - \prod^{N} (1 - P_i).$$

## 1.6 Long-Range Forecast Procedure:

As a first approximation to the five-day flare prediction the forecaster assumes that the current 24-hour prediction is valid and that conditions on the sun will not change during the 5-day period. Then, the probability of at least one event in the 96-hour forecast period (hour 24 through hour 120) is given by

$$P_{24-120} = 1 - (1 - P_{0-24})^4.$$

This function is illustrated in Figure 1-4, below:

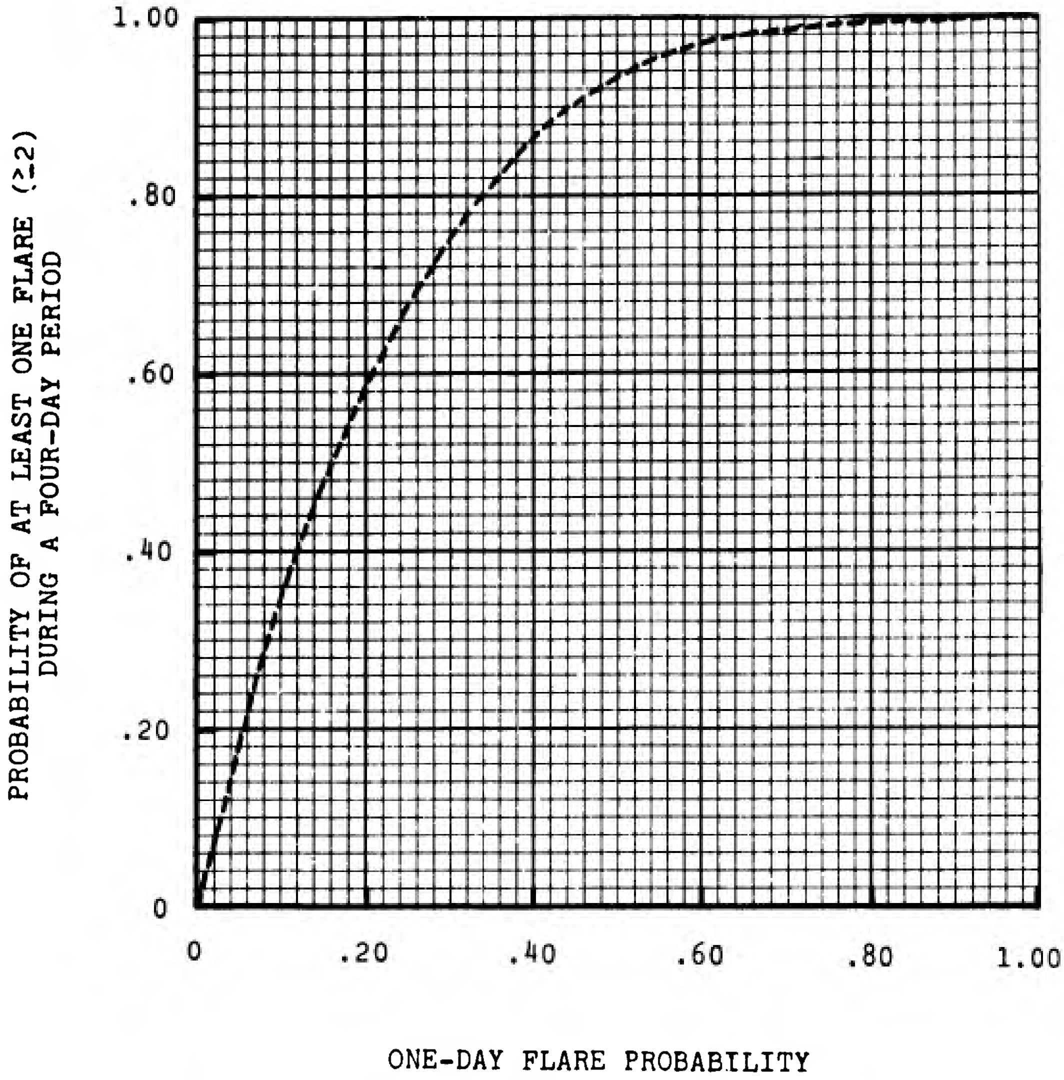


Figure 1-4

This computed probability is then adjusted subjectively by considering activity trends of visible active regions, east-limb indications of returning active regions, active regions about to rotate over the west limb, and active regions which are due to return within the 96-hour forecast period.

In situations where large changes in the one-day flare probability are expected during the four-day forecast period, use of the following formula is recommended:

$$P_{24-120} = 1 - \prod^{4} (1-P_d)$$

where $P_d$ is the best estimate of one-day flare probability for each of the four days of the forecast period.

# Chapter 2

## PROTON EVENT FORECAST

2.1 Proton-Event Forecast Format and Definitions:

a. Proton-Event Definition. A "proton event" is defined as the arrival at the earth of a detectable number of solar protons having energy greater than 20 Mev. The occurrence of a proton event is normally verified by satellite observations or by a Polar Cap Event (PCE).

b. SFC Forecasts. A color-coded forecast scheme referring to the beginning of a proton event is issued by the SFC. The code word "PESTF" is used for all proton-event forecasts.

c. PESTF GREEN. "PESTF GREEN" means that a proton event is not expected. Too few indicators favorable to the occurrence of a proton flare are observed on the sun.

d. PESTF YELLOW. "PESTF YELLOW" means that a proton event is considered likely if a major flare should occur. This requires the existence of optical and/or radio indicators favorable to the occurrence of a proton flare.

e. PESTF RED. Once a major flare has occurred, all available data are examined by the forecaster to determine the likelihood of a proton event. "PESTF RED" means that a proton event is likely to begin before a specified time although some indicators may be missing; the probability of a proton event is greater than thirty percent.

f. PESTF PURPLE. The establishment of a "PESTF PURPLE" requires the existence of additional information (over and above that necessary for a "PESTF RED") which confirms both proton emission and the likelihood of proton interception by the earth. The probability of a proton event is greater than sixty percent.

2.2 General. As with the flare predictions described in Chapter 1, the procedure for proton-flare forecasting is based on analyses of individual active regions. The specific procedure used at the SFC is designed to contribute directly to the "Proton-Event Start-Time Forecast" (PESTF) format: i.e., the decision to establish a "PESTF YELLOW" is based on a pre-flare analysis, and decisions on "PESTF's RED and PURPLE" are based on immediate post-flare analysis of selected parameters. Both pre-flare and post-flare analyses are described below.

2.3 Pre-Flare Evaluation. The attached work sheet (Figure 2-1) lists characteristics of solar active regions which contribute to proton-flare prediction and which are normally available at the SFC. The work sheet assists the forecaster in his subjective evaluation of each active region. The standard procedure for evaluating the likelihood of a proton-flare is as follows:

A. Regions must meet three basic conditions:

(1) Requires Active Region History Chart (see paragraph 1.4c).

(2) Plage area at least 3500 millionths of the solar hemisphere.

(3) Plage brightness at least 3.0.

B. A REGION INDEX is then determined (See Figure 2-1):

(1) The forecaster enters each predictor line with the current value of that predictor; he either circles the value (if it is pre-printed) or he enters the current value at the appropriate position.

(2) The INDEX for each parameter is determined and is listed in the far right-hand column; the indices are summed and a mean index is computed.

C. In addition to computing the REGION INDEX, the forecaster considers the distribution of the parameters in a "FAVORABLE/UNFAVORABLE" listing; parameters whose indices are greater than 3.9 are considered "FAVORABLE" --- all others are listed in the "UNFAVORABLE" column.

D. The final decision on whether to establish a "PESTF YELLOW" is subjective and rests with the judgement of the forecaster. The REGION INDEX and the "FAVORABLE/UNFAVORABLE" distribution are used as guides. For example, the simultaneous existence of a REGION INDEX greater than 3.5 and a parameter distribution showing 70% of the available predictors in the "FAVORABLE" column would usually result in a decision to establish a "PESTF YELLOW" condition.

Studies are in progress at the SFC to improve the subjective placement of indices and to determine weight factors for each of the listed predictors so that the evaluation may be carried out as in Chapter 1. Each of the parameters listed in Figure 2-1 is described below.

a. Calcium Plage Area. Although proton flares are usually associated with large, bright, flare-rich plages, only a few such plages actually produce proton flares. Of the 520 McMath numbered plages in 1957, 78 (15%) produced major solar events, but only 13 (2.5%) produced all 17 Polar Cap Events (PCE's) observed in that year

| SFC REGION ______ DATE ______ | INDEX 0 | 1 | 2 | 3 | 4 | 5 | 4 | |
|---|---|---|---|---|---|---|---|---|
| CA PLAGE AREA | | | | 4000 → | 5000 → | | | |
| PLAGE BRIGHTNESS | | | | | 3 | 3.5 | | |
| PLAGE AGE | 7 | 6 1 | 5 4 | | 3 | 2 | | |
| SPOT MAG CLASS | | α | | β | βγ | γ, δ | | |
| SPOT ZURICH CLASS | A B C | D | J G | H | E | F | | |
| SPOT AREA | 200 | | 300 | | 500 → | | | |
| DISK POSITION | 90E | | 45E | | | CM | 90W | |
| SEASON | 1 Dec-20 Jan | 20 May-20 Jun | | OTHER | | Mar, Aug Apr, Sep | | |
| RADIO FLUX DEVIATION ($10^{-22}$ w/m$^2$ cps) | | | -20 | 0 | 50 | 80 | | |
| RADIO BRIGHTNESS ($10^3$ °K) | | 200 | | 500 | | 1000 | | |
| | | | | | TOTAL | | | |
| | | | | | REGION INDEX | | | |

| FAVORABLE | UN-FAVORABLE |
|---|---|
| | |
| | |
| | |
| | |
| | |
| | |
| | |
| | |
| | |
| | |

Figure 2-1. Pre-Flare Evaluation Work Sheet

[Sherry, 1966]; similarly, for the period 1954-1963, 40 plages produced 59 PCE's. The distribution of plage size and PCE production is as follows [Jonah, 1966]:

| | | | |
|---|---|---|---|
| MEAN PLAGE AREA | > 4000 | > 5000 | > 6000 |
| TOTAL # OBSERVED | 328 | 224 | 172 |
| # PRODUCING PCE's | 36 | 29 | 27 |
| % PRODUCING PCE's | 11 | 13 | 16 |

b. Calcium Plage Brightness. The McMath brightness of every PCE plage was at least 3.0 [Jonah, 1966].

c. Plage Rotation Age. Thirty-five of the 40 PCE plages listed by Jonah [1966] were in their 2nd or 3rd rotation. The following table shows the PCE plages listed by rotation age and hemisphere. (Plages which were composites of different ages, excluding two first-rotation plages, are listed by the youngest age.)

| ROTATION | 1 | 2 | 3 | 4 | 5 | 6 | TOTAL |
|---|---|---|---|---|---|---|---|
| NORTH | 1 | 13 | 10 | 2 | 1 | | 27 |
| SOUTH | | 7 | 5 | | | 1 | 13 |
| TOTAL PLAGES | 1 | 20 | 15 | 2 | 1 | 1 | 40 |

It should be noted that of the approximately 4000 plages reported from late 1954 through 1963, only 110 plages returned for an active 2nd disk passage, and 77 returned for an active 3rd disk passage; therefore, 18% of all 2nd-rotation active plages and 19% of all 3rd-rotation active plages produced PCE flares. Only one of the 4000 plages reported produced a PCE during the 1st-rotation.

d. Spot Magnetic and Zurich Class. The following table illustrates the distribution of PCE flares by spot magnetic class and Zurich class [Jonah, 1966]. Note that E-type spot groups were observed slightly over 4 times more frequently than F-type groups during the period under consideration; E groups produced only about 3 times as many PCE flares as did F groups, indicating that the F classification may be slightly more significant. Similarly, beta-gamma spot groups were observed nearly 2.5 times more frequently than gamma groups during the period examined by

Jonah; beta-gamma groups produced only 1.5 times as many PCE's as did gamma groups, indicating that the beta-gamma classification may be more significant.

| MAGNETIC CLASS | ZURICH CLASS | | | | | | | | | |
|---|---|---|---|---|---|---|---|---|---|---|
| | A | B | C | D | E | F | G | H | J | TOTAL |
| GAMMA | | | | | 7 | 2 | | 6 | | 15 |
| BETA-GAMMA | | | | | 14 | 6 | 2 | | | 22 |
| BETA | | | 1 | 3 | 8 | 1 | 1 | 1 | | 15 |
| ALPHA | | | 1 | | | | 1 | | 3 | 5 |
| ??? | 1 | | | | | | | | 1 | 2 |
| TOTAL PCE's | 1 | 0 | 2 | 3 | 29 | 9 | 4 | 7 | 4 | 59 |

The placement of the delta configuration in Figure 2-1 is based on an article by Warwick [1966]. In the actual use of the work sheet, any spot group which was once reported as complex is rated as a complex group as long as it is on the disk; that is, a group now rated as a beta but which had been a beta-gamma or gamma will not receive an index less than 4.0.

e. Spot Area. Analysis of PCE data given by Jonah [1966] gives the following distribution of PCE flares with spot area (spot group frequency obtained from Jonah, Dodson-Prince, and Hedeman [1965]:

| SPOT AREA (millionths of the solar hemisphere) | Under 500 | 500-1000 | Over 1000 |
|---|---|---|---|
| TOTAL # SPOT GROUPS OBSERVED WITH MEAN AREA WITHIN GIVEN LIMITS | ? | 318 | 153 |
| # GROUPS PRODUCING PCE's | 4 | 17 | 20 |
| # PCE FLARES PRODUCED (six PCE flares were associated with spot groups for which data are not available.) | 4 | 19 (32%) | 30 (51%) |

Although there are no conclusive statistics available at the present to relate PCE occurrence with spot growth, flares are most frequently observed in rapidly-growing regions [Warwick, 1965].

f. Disk Position. The following illustrates the distribution of PCE flares over the solar disk during the period late 1954 through 1963 [Jonah, 1966]:

| CENTRAL MERIDIAN DISTANCE | 90°E | 45°E | CM | 45°W | 90°W | TOTAL |
|---|---|---|---|---|---|---|
| NORTH | 4 | 10 | 13 | 9 | | 36 |
| SOUTH | 3 | 8 | 7 | 5 | | 23 |
| TOTAL | 7 | 18 | 20 | 14 | | 59 |

g. Seasonal Variation. Figure 2-2 is a graph of PCE's taken from various sources showing the seasonal variation of PCE observations. Note the apparent maxima near the equinoxes and minima near the solstices (the minimum near the summer solstice is more apparent in major-event observations).

h. 10-cm Flux Deviation. Seventy-four percent of the 59 PCE's listed by Jonah [1966] occurred when the daily 10-cm flux value prior to the PCE flare was above the 90-day running mean ending on that day; this is illustrated in Figure 2-3. (A study of major flares during 1966 shows that 90% occurred when daily flux values were above the 90-day running mean [Tudor, 1966].)

i. Radio Brightness Temperature. The Stanford 9.1 cm radio brightness temperature is included as a predictor even though correlation studies have not been completed. Placement of brightness temperatures in specific index ranges is based on a subjective evaluation with reference to brightness/flare-production relationships.

j. Other Predictors. Personnel at the SFC are engaged in local studies involving other predictors. Spot growth, spot age, heliographic longitude, filament configuration and activity, and flare activity are the additional parameters now being evaluated for their relationships with major flare and PCE production.

THE BI-ANNUAL VARIATION OF PCA EVENTS FROM 1942 - 1966

Number of
PCA Per 10
Day Periods

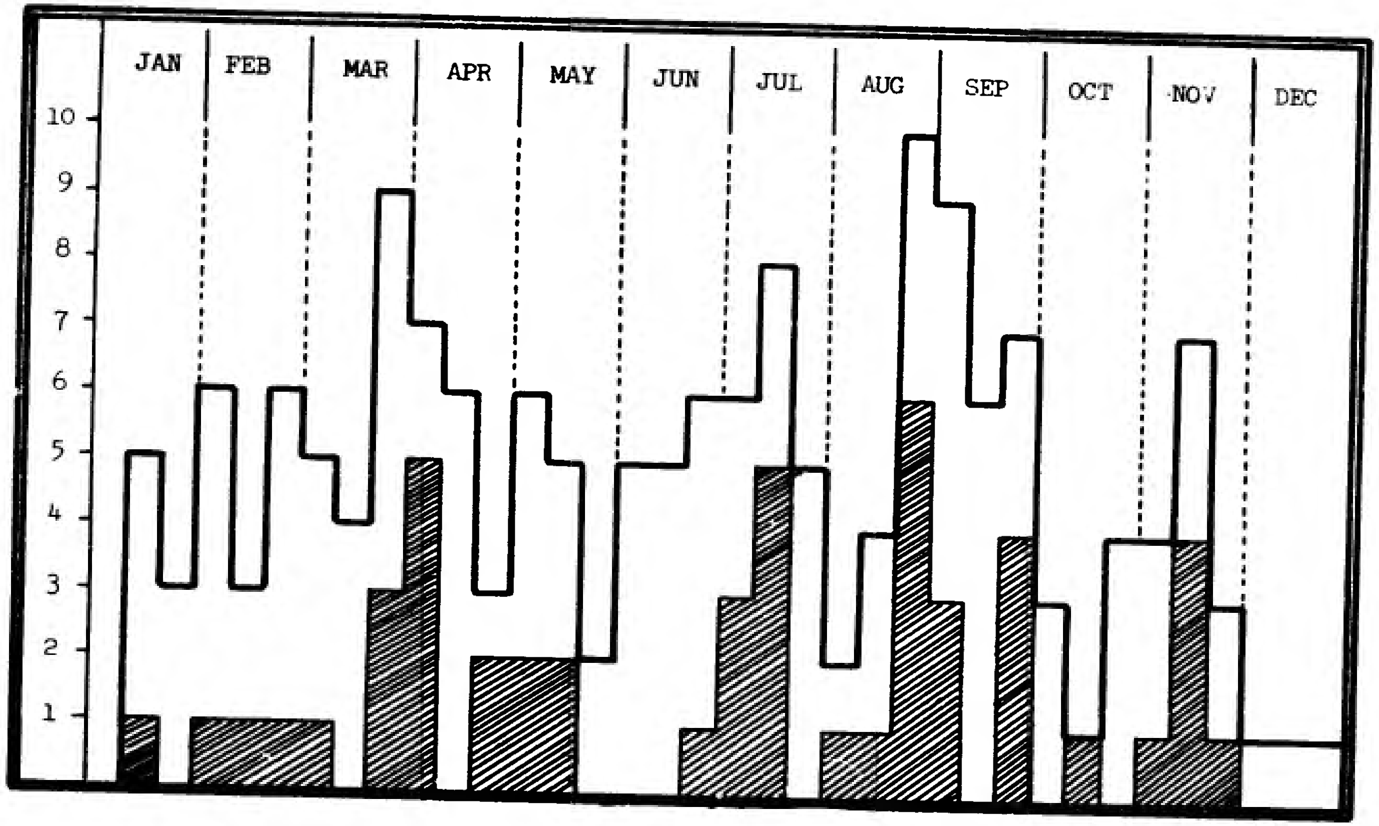


Principle
References:

Jonah, 1965
McDonald, 1963
Gnevyshev and
Kriusky, 1966

LEGEND:

Hatched Graph Depicts Major PCA

(None detected late May - early June; December to early January)

Solid Graph Depicts ALL PCA

(None detected early January)

Figure 2-2.

DISTRIBUTION OF PCA EVENTS

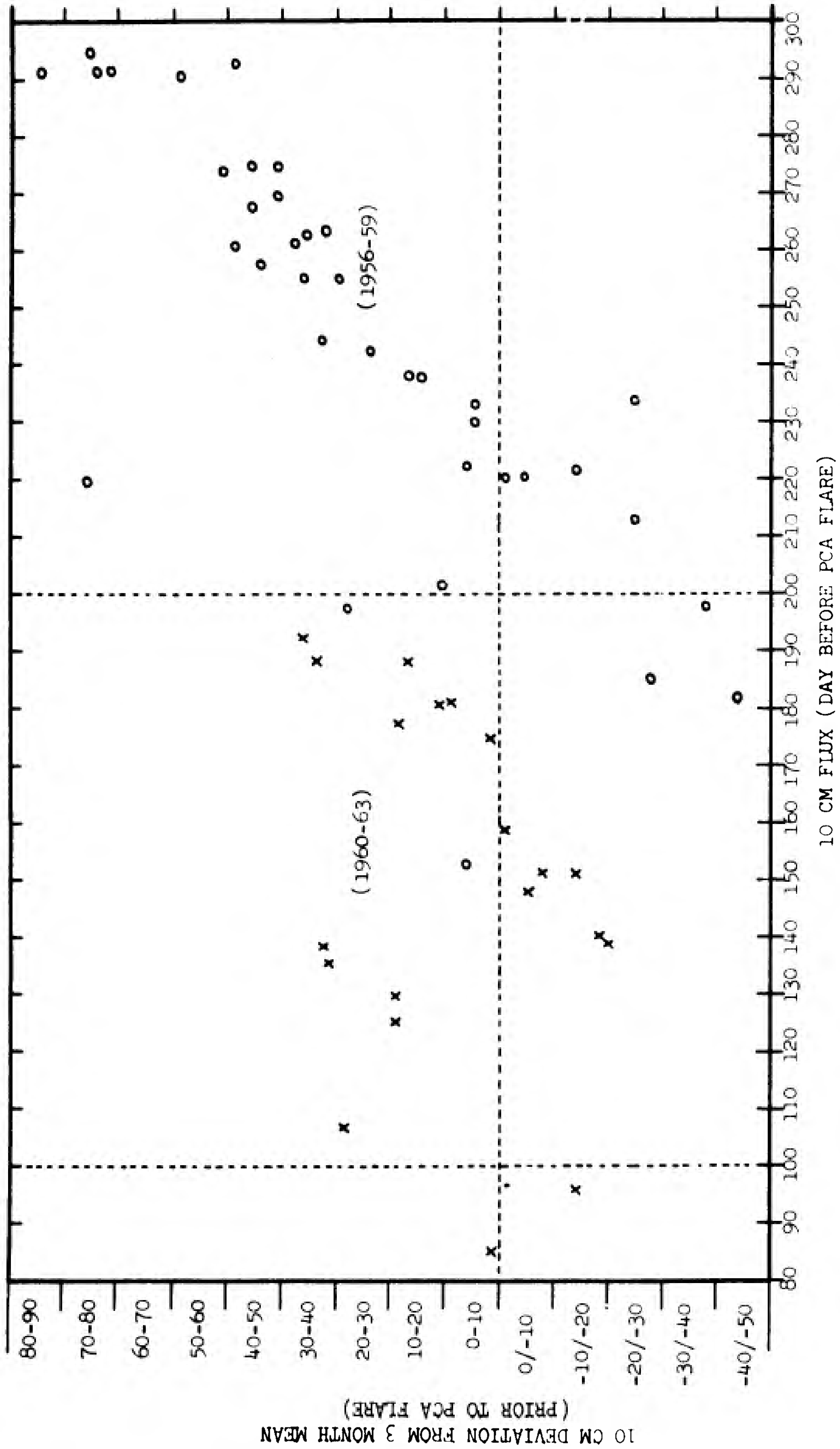


Figure 2-3.

2.4 Forecasting a Proton Event After a Major Flare Occurs:

a. This section will consider forecasting those proton events which are detectable in the vicinity of the earth, given that a flare of at least Importance 2 has been optically observed. Most of the pre-flare characteristics considered in the previous section are also important in post-flare analysis.

b. Once the optical flare is observed and reported, the forecaster has little time to make a firm proton event forecast. Particles may begin arriving at the earth within a half hour, but may be delayed several hours. The delay time between the optical flare onset and the arrival of particles rarely exceeds 18 hours; the average delay time is approximately 4 hours [SFC, 1966]. Figure 2-4 has been designed by Center personnel to assist the forecaster in making a rapid proton event forecast. This figure incorporates pre-flare characteristics as well as the major-flare-associated characteristics which sometimes accompany large flares. The figure represents an accumulation of statistics which can be compared and used to calculate a proton event forecast.

c. Once the large optical flare occurs, the detection of particles at the earth depends very heavily upon the configuration and strength of the geo- and interplanetary magnetic field. The radio events associated with the optical flare, as well as the position of the flare on the disk, provide the most reliable tools to forecast this detection (Figures 2-4, 2-5 and 2-6). Figure 2-5 is adapted from data listed in NASA Program Apollo Working Paper No. 1193 [1966]. Figure 2-6 is based on a short term proton event prediction method using Type IV radio bursts and flare disk position [SFC, 1965]. The four recorded cases of large white light flares during the period 1958-1963 which are listed by Bruzek [1964] as all being associated with proton events are too few to be a reliable predictor. Reports of loop prominence systems on the solar disk and west limb offer a fairly reliable predictor; however, Bruzek's tables list only 20 limb loop systems and 25 disk loop systems during the period November 1956 through September 1963.

d. As a general rule, the larger the solar flare, the stronger will be its associated radio events. Proton events are much more likely to be associated with the larger flares and stronger radio events. However, it is generally not sufficient

| | | PCA EVALUATION AFTER FLARE OF IMPORTANCE ≥ 2 | | | | | | | | | | | | REFERENCE |
|---|---|---|---|---|---|---|---|---|---|---|---|---|---|---|
| | | 0%–5 | 5–10 | 10–15 | 15–20 | 20–30 | 30–40 | 40–50 | 50–60 | 60–70 | 70–80 | 80–90 | 90–100 | |
| 1 | Flare Importance | Imp 2 <1% | | | | Imp 3 | | | | | Imp 4 | | | Jonah, Dodson-Prince, Hedeman, 1965 Smith & Smith, 1963 |
| 2 | Preflare Index | <2.5 | | 2.5–2.9 | | | 3.0–3.9 | | 4.0–4.9 | | | | 5.0 | SFC Unpublished Forecast Study |
| 3 | Flare Importance and Type IV | Imp 1 | | | | | Imp 2 | | Imp 3 | | | Imp 4 | | SFC Unpublished Forecast Study |
| 4 | Location of Flare with Type IV | | | | | | 90E–30E | 30E–CM 90W–20W | CM–20W | | | | | SFC Unpublished Forecast Study |
| 5 | Flare and 10 cm Burst ≥ 500 | | 10 cm max preceeds Hα max | | | 10 cm burst only | | | | | 10 cm max follows Hα max | | | Dodson and Hedeman, 1964 |
| or | Flare, 10 cm Burst ≥ 500 and Type IV | 10 cm max preceeds Hα max, no Type IV | | | | 10 cm max preceeds Hα max & Type IV | | | | 10 cm max follows Hα max & Type IV | | | | Dodson and Hedeman, 1964 |
| 6 | Broad cm, Type II, IV & Disk Position | | | | | | | Eastern Hem | | | Western Hem | | | Harvey, 1965 |
| 7 | Broad cm, no II, and Disk Position | | | | | Eastern Hem | | | Western Hem | | | | | Harvey, 1965 |
| 8 | Loops | | | E Limb | | | | W Limb | | Ern Hem | | Wrn Hem | | Bruzek, 1964 |
| 9 | Flare Filament | | | V or Y | | Parallel | | | | | | | | Warwick, 1965 |
| 10 | Umbra Covered | | | | | | | | | | | | | Dodson and Hedeman, 1964 |
| 11 | White Light Flare | | | | | | | | | | | Disk or Limb | | Bruzek, 1964 |
| 12 | Region Previously Produced Protons | | Current Rotation | | | | Current & Previous Rotation | | | | | | | SFC Unpublished Forecast Study |

Figure 2-4.

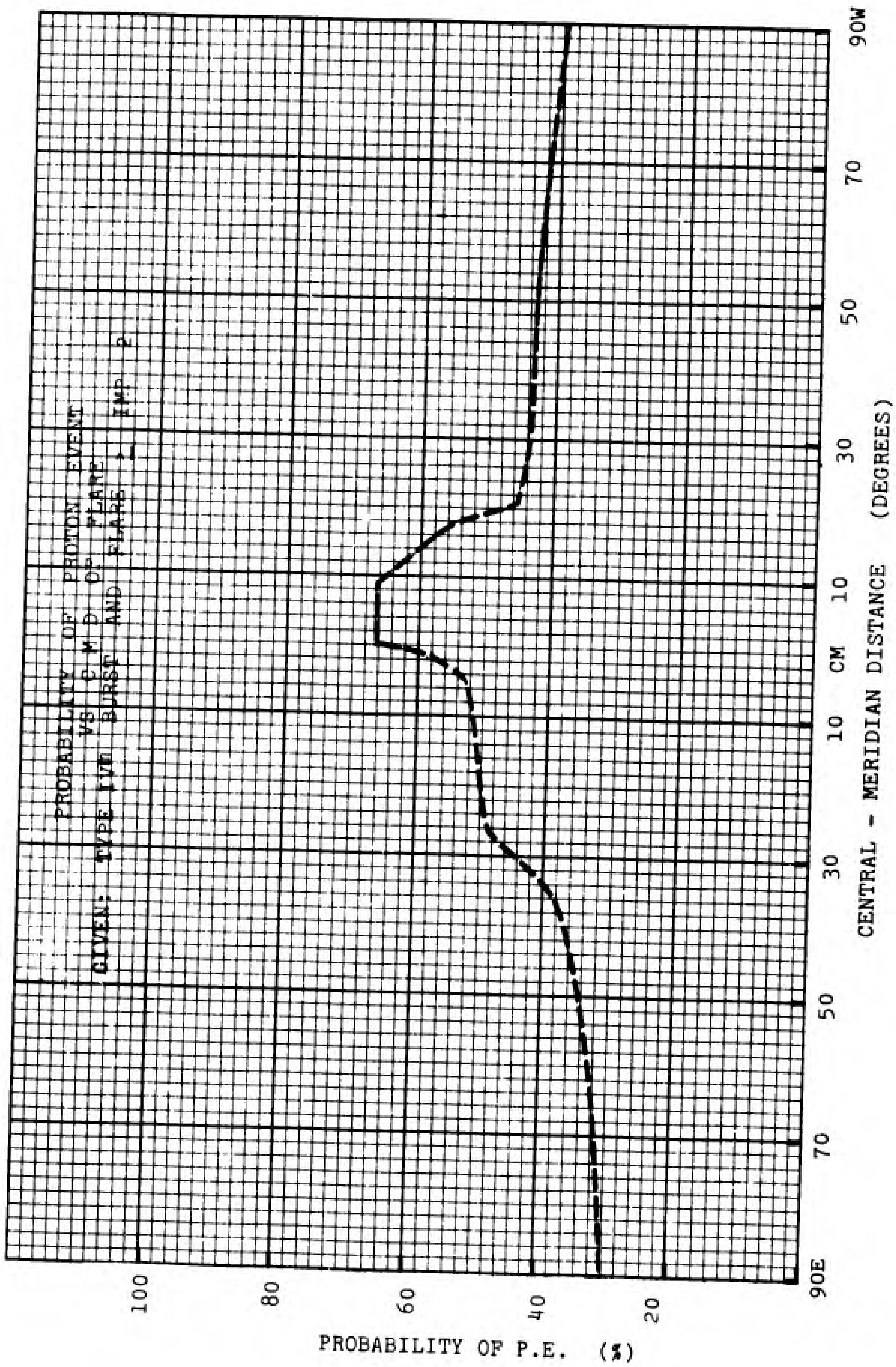
PROBABILITY OF PROTON EVENT
VS C M D OF FLARE
GIVEN: TYPE IV/II BURST AND FLARE ≥ IMP 2
90W
70
50
30
10
CM
10
30
50
70
90E
CENTRAL - MERIDIAN DISTANCE (DEGREES)
100
80
60
40
20
PROBABILITY OF P.E. (%)

Figure 2-5.

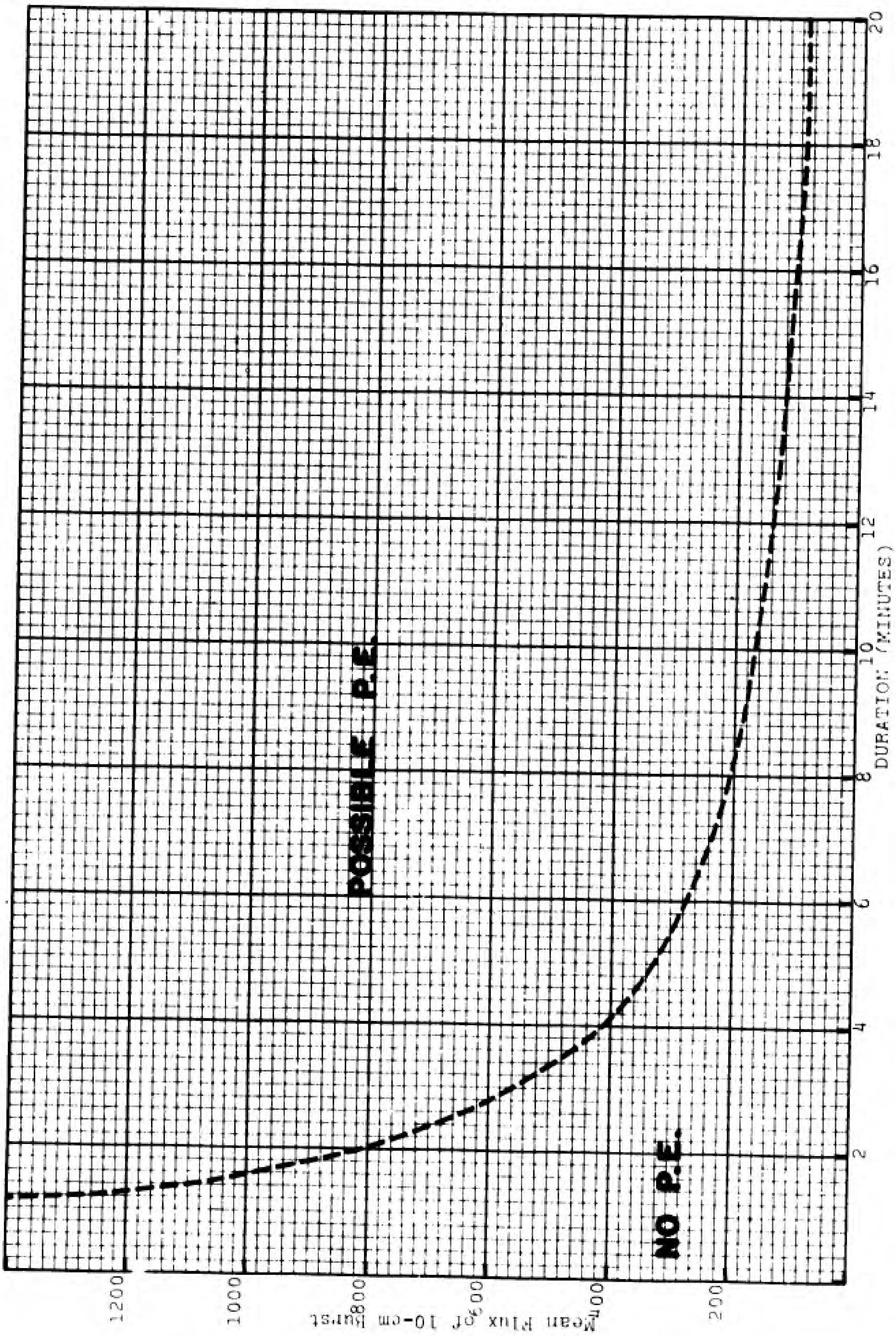
POSSIBLE P.E.
NO P.E.
2
4
6
8
10
12
14
16
18
20
DURATION (MINUTES)
200
400
600
800
1000
1200
Mean Flux of 10-cm Burst

Figure 2-6.

to have only the flare and one other predictor to make a successful forecast. In fact, Dodson and Hedeman [1964] found the only sufficient condition for a proton event to be the simultaneous occurrence of an Importance 4 flare covering large umbra, great Type IV emission and great 10-cm burst with maximum after the H-alpha maximum.

e. Figure 2-4 is used anytime a flare of Importance 2 or greater is reported. As soon as one of the predictors, $P_n$, is known, a percentage for that predictor is assigned. (Note: Either $P_1$ or $P_3$ will be used as a predictor, depending on whether or not a Type IV radio burst has been reported.) The predictors are not weighted. A final percentage $\overline{P}$ is assigned using the formula:

$$\overline{P} = 1 - \prod^{n} (1 - P_n).$$

f. After $\overline{P}$ is calculated, the solar forecaster applies the result in determining the color coded Proton Event Start Time Forecast (PESTF).

THIS IS A BLANK PAGE

Chapter 3

## FORECASTING THE 10-cm SOLAR RADIO FLUX

3.1 General. Superimposed upon the steady thermal emission from the quiet sun, there is a component which shows daily variation. This slowly varying or S-component is revealed in measurements at centimeter and decimeter wavelengths and is correlated with total sunspot area. In general the 10-cm flux under quiet sun conditions originates in the chromosphere. When active regions are present the slowly varying component is introduced and its source is considered to be the lower corona.

3.2 Type of Variations in the S-Component. The S-component of the 10-cm radio flux is produced in the corona above active regions. The variations in the intensity of this flux can be divided into three types which are related to changes of the active regions. These are:

Type I: Center-to-limb variation
Type II: Large-scale variation
Type III: Small-scale variation

a. Type I, Center-to-Limb Variation. Due to the anisotropy of the solar emission at decimetric wavelengths, the movement of active regions across the solar disk produces variations in the flux recorded at the earth. Figure 3-1 shows the center-to-limb variation for a strong, moderate, and weak source at 9.1 cm [Swarup, 1963]. (The flux density is: strong > 15, moderate 8-15, weak 3-8, in units $10^{-22}$ $w/m^2$ cps.)

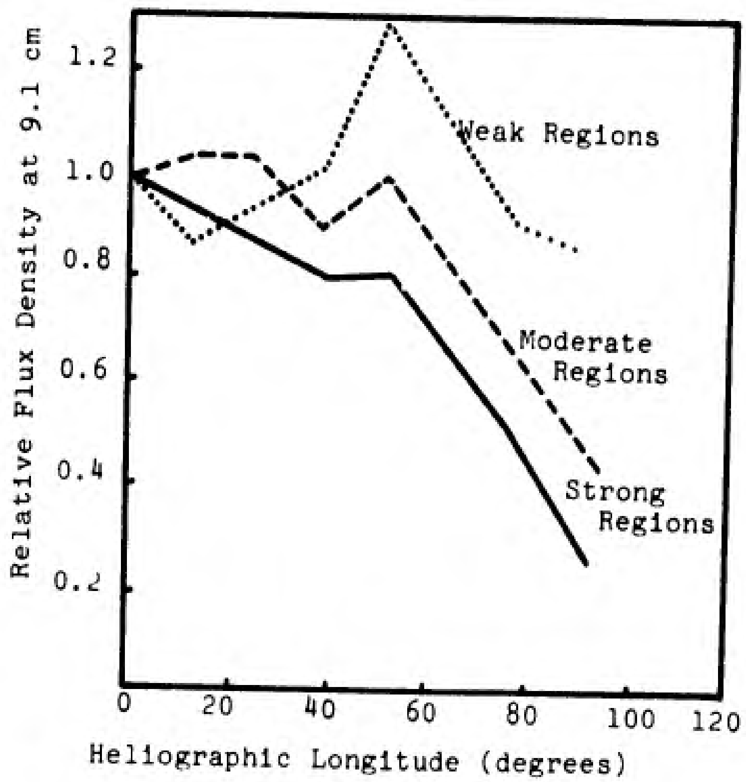


Figure 3-1. Center-to-Limb Variation [Swarup, 1963]

There is no ambiguity in using this graph for regions passing from central meridian (CM) to the west limb; however, an independent strength determination must be made when the region first appears on the east limb. (Flux values which determine the strength are CM values.) This determination is made from optical observations at the limb, that is, strength of coronal line emission, plage size and intensity, sunspot size and type, and surge and prominence activity.

b. Type II, Large-Scale Variation. As an active region progresses through its life cycle, its sunspot area and magnetic field increase to a maximum and then decrease. The flux emitted from the region shows a similar variation. A typical sunspot growth curve is shown in Figure 3-2.

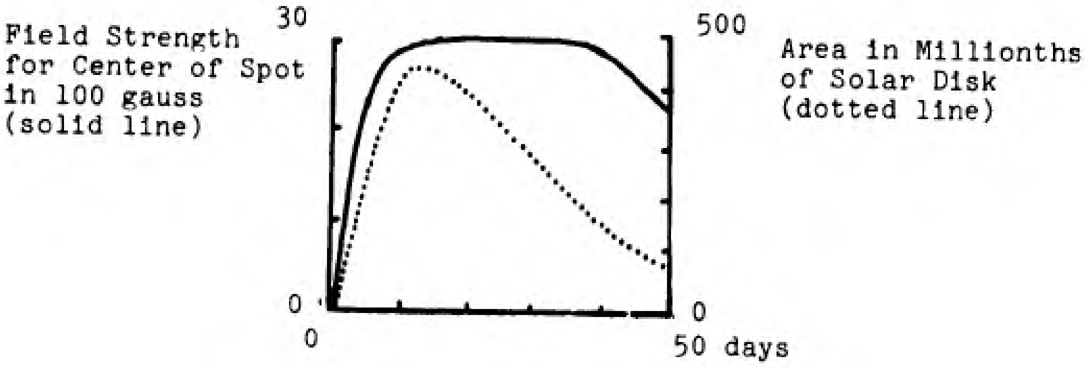


Figure 3-2.

An area-growth curve (Figure 1-2) for each active region can be extrapolated following the basic form presented in Figure 3-2, to provide future values of sunspot area. Generally, this type of variation is fairly continuous (within the limits of observation) and extrapolation is feasible.

c. Type III, Small-Scale Variation. This type of variation is short-term (about 1 to 4 days) and is superimposed on the long-term changes discussed above. This type of flux increase is probably produced by increased turbulence and electron thermal velocity within the active region. Unfortunately, there are currently no methods to anticipate these rapid changes. A forecaster must, however, recognize this type of change in order to prevent overforecasting by misinterpreting these short-term changes as indicative of long-term variations. Type III variations have the following characteristics:

(1) They are sudden and do not correlate with sunspot growth or movement.

(2) The active region usually shows other signs of increased turbulence, e.g., flares and/or subflares, surges, and active filaments.

3.3 Regression Equations. When major regions are present on the disk, the existing trend and the above sections should receive major consideration. For other periods, and as a guide, various regression equations are available. The following set, developed by the Traveler's Research Center, Inc., under the auspices of Air Force Cambridge Research Laboratories (AFCRL), is used daily at the SFC.

a. 1-day forecast:

$$F_1 = 0.7687 + 1.0929F_0 - .0454F_{-1} - .0951F_{-3} - .0375F_{-4} - .0211F_{-13} + .0015F_{-19} + .0429F_{-23}$$

b. 2-day forecast:

$$F_2 = 1.6063 + 1.1315F_0 - .1432F_{-2} - .1173F_{-3} - .0499F_{-4} - .0499F_{-12} + .1162F_{-14} + .0224F_{-19} + .0793F_{-23}$$

c. 3-day forecast:

$$F_3 = 2.5208 + 1.2188F_0 - .1516F_{-1} - .1442F_{-2} - .1924F_{-3} - .0399F_{-11} + .1426F_{-14} + .0224F_{-19} + .1271F_{-22}$$

Where $F_1$, $F_2$, and $F_3$ are forecast values for days 1, 2, and 3; $F_0$ is the flux and the day the forecast is issued; $F_{-1}$, $F_{-2}$, .... are observed values on the past appropriate days in the past.

THIS IS A BLANK PAGE

# Chapter 4

## FORECASTING GEOMAGNETIC ACTIVITY

4.1 The Forecast of Geomagnetic Disturbances. A magnetic disturbance has at least five major components and many associated physical effects.

a. Major Components of a Magnetic Disturbance D. [Cole, 1966].

D = DCF + DR + DT + DI + DG.

A magnetic disturbance has at least five major components which result from:

(1) Currents caused by solar corpuscular flux interacting with the earth's magnetopause (DCF).

(2) One or more magnetospheric ring currents (DR).

(3) Magnetospheric tail currents (DT).

(4) Ionospheric currents (DI).

(5) Induced ground currents (DG).

The DCF and DT effects are always present, however they are enhanced at times of sudden commencements and polar magnetic substorms, respectively. Magnetograms from equatorial and polar regions show the DR and DI effects, respectively. Ground currents have been detected, and they must share in the total disturbance.

b. Physical Effects Associated With a Magnetic Disturbance. The following are direct and indirect effects associated with a magnetic disturbance [Cole, 1966]. Not all the effects are necessarily expected with every disturbance.

(1) Depression of the geomagnetic field at the equator.

(2) Polar magnetic bays.

(3) Irregular magnetic activity.

(4) Gradual or Sudden Change (GC or SC) in the level of the magnetic trace.

(5) Active aurora or enhancement of the quiet aurora.

(6) Stable auroral red arcs.

(7) Change in the structure of the ionosphere.

(8) Heating of the upper atmosphere.

Magnetic bays are transient departures of the magnetogram trace from normal. The average duration of the departure is one half to one hour.

c. Great Geomagnetic Storms. Geomagnetic disturbances or storms are usually classed according to the value of $A_p$,

No storm: $A_p$ <25

Small storm: $A_p \geq 25$

Moderate storm: $A_p \geq 50$

Great storm: $A_p \geq 100$ and/or $K_p \geq 9-$.

Great geomagnetic storms are usually associated with a major solar flare. For this reason the precursors to a great geomagnetic storm are usually well marked. The list that follows represents the ideal conditions for a categorical YES forecast for a great geomagnetic storm.

(1) An importance 2 or greater solar flare that occurred
  (a) within $45^o$ of the central meridian
  (b) in the northern hemisphere
  (c) in a magnetically complex spot group

(2) A type IV radio burst that was
  (a) over cm and meter wavelengths
  (b) at least 15 minutes in duration
  (c) preceded by a type II burst

(3) A polar cap absorption event

The first two conditions can be evaluated at the time of the flare occurrence. The polar cap absorption, which normally occurs within 10 hours of the solar flare, should serve to strengthen the certainty of the forecast made on the basis of the first two conditions.

There is evidence that the northern hemisphere of the sun has been the most probable source of great geomagnetic storms during the 20th century. However, in the last half of the 19th century the southern hemisphere was the more active in the production of great storms. It is not possible to predict when the northern hemispheric preference will wane in favor of the southern.

The delay time between the start of a "proton flare" and the start of the PCA may be used to estimate the start time of the geomagnetic disturbance. SFC personnel have added data to those considered by Warwick [1963] and now forecast a SC disturbance to begin (0.73t + 20) hours after the start of the PCA-associated flare (t is the time in hours between the start of the flare and the start of the PCA). For PCA delay times of less than ten hours, the above expression gives the earliest expected geomagnetic-disturbance start time. The geomagnetic disturbance may be expected to start 20 to 40 hours after the associated flare; the most probable delay time is about 36 hours.

d. M-Region Storms. In contrast to the sudden commencement geomagnetic storms, which are flare-associated and non-recurrent, gradual commencement storms are associated with localized "M (magnetic) -regions" [Bartels, 1934], which seem to be fixed locations on the sun that emit streams of plasma and recur with about a 27 day periodicity. Although they occur throughout the solar cycle, M-regions are most common in the two to three years before solar minimum. There are differing opinions as to whether or not M-regions are related to optical features such as plages or sunspots. It has also been suggested that they are related to the remains of formerly visible features. The plasma from M-regions can usually be distinguished from the undisturbed solar wind by the plasma's higher velocity.

The recurrent nature of M-region storms is a useful forecast tool, but it involves several difficulties:

(1) There is no assurance that an M-region disturbance will return, although they usually do.

(2) If they do return, they often appear after 28 days instead of the expected 27, and occasionally they return a day early.

(3) The size of a returned disturbance only roughly approximates its size in the previous solar rotation.

e. Lunar and Planetary Influences. Several researchers have sought to correlate lunar and/or planetary phase with geomagnetic activity. Such individuals are confronted with the two-fold task of establishing their results as statistically significant and of suggesting a plausible physical explanation of their results. The literature provides a variety of conclusions, some contradictory, yet each regarded by its author as statistically sound.

One author, [Bigg, 1963], used magnetic data from 1874 to 1958 and discovered a decrease in geomagnetic activity within two days of new moon and within two days of inferior conjunction of Mercury and of Venus. In each of these cases the moon, Mercury, or Venus would be near the earth-sun line. Bigg postulated that the geomagnetic field is partially shadowed from the solar wind by the intervening body. This shadow effect causes a decrease in geomagnetic activity. Bigg also reported that there is an increase in magnetic activity within one day after full moon and that magnetic storms are more frequent when the earth is near the equinoxes. Using data from 1932-1959, [Stolov, 1965] and [Bell and Defouw, 1966] found a decrease in geomagnetic activity before full moon and an increase after full moon. This effect was most apparent when the celestial latitude (or angular distance from the plane of the ecliptic) of the full moon was small. When the celestial latitude, B, taken without regard to sign, is less than one degree, the lunar effect is greatest. For angles of one to four degrees from the ecliptic the effect is somewhat less, and the minimum and maximum activity occur about a day later. For over four degrees up to the largest possible angle of just over five degrees, the effect is not apparent.

The proposed explanation for this lunar modulation of geomagnetic activity involves the geomagnetic tail, which is discussed in Attachment 2. The tail lies approximately in the plane of the ecliptic, along the earth-sun line. Satellite measurements have established that it extends well past the moon's orbit. For small celestial latitudes of the full moon, the moon passes through the center of the tail where interactions may occur that propagate back to the earth.

Complications in the concept of lunar modulation of the geomagnetic field arose when a study of magnetic data from 1889-1932 (solar cycles 13-16) did not show the significant variation of activity around full moon that appeared in the 1932-1959 data (cycles 17-19). However, the effect did seem to be present once again in the 1884-1889 data (cycle 12). At least two conclusions may be inferred: the length of the magnetic tail varies markedly with the 80-year solar cycle; or the detection of lunar modulation in some of the data was a statistical fluke.

The questionable statistical significance of lunar and planetary influences on geomagnetic activity is not likely to be resolved until the physical mechanisms involved are more firmly established. Furthermore, if one assumes that the lunar modulation at full moon is a valid forecast technique only during alternate periods of four solar cycles each, the technique will be effective only until the end of cycle 20, about 1975. It will then be another 44 years before the lunar modulation of geomagnetic activity again becomes effective.

f. Other Forecasting Techniques. A method of forecasting small magnetic disturbances is currently under study at the Solar Forecast Center. Preliminary results indicate that a sufficient change in the ratio of the 8800 MHz solar radio flux to the 2695 MHz flux usually precedes a geomagnetic disturbance of $A_p \geq 10$ by about three or four days. Changes in the ratios of the fluxes at other frequencies are also being investigated. This "flux ratio" technique seems to be fairly successful in forecasting disturbances which had not appeared in the sun's previous rotation. In addition, the method can lend support to predictions that a given M-region disturbance will return.

A quantitative forecast technique is also under study to forecast the occurrences of $A_p \geq 50$ and $A_p \geq 100$. The preliminary work has yielded the following approach to the problem:

PRELIMINARY TECHNIQUE FOR THE FORECAST OF

LARGE GEOMAGNETIC DISTURBANCES

| CRITERIA | YES | NO |
|---|---|---|
| Did a flare occur of importance TWO or greater? | 9 | 0 |
| Did the flare occur in the northern hemisphere? | 7 | 0 |
| Did the flare occur within 45° of the central meridian? | 7 | 0 |
| Did the flare occur in a β, βγ, γ or δ spot group? | 7 | 0 |
| Did a type II radio burst occur? | 10 | 0 |
| Did a type IV radio burst occur? | 11 | 0 |
| Did the type IV burst occur for ≥ 15 minutes? | 11 | 0 |
| Did the type IV burst occur over cm and m wavelengths? | 11 | 0 |
| Did a type II radio burst precede a type IV burst? | 14 | 0 |
| Did a PCA occur? | 13 | 0 |
| Total G | 100 | 0 |

INSTRUCTIONS: Enter the above table and answer the questions either yes or no. Total the corresponding YES occurrence values. If the total, G, is $45 \leq G < 60$ forecast $50 \leq A_p < 100$ for the second day following the flare. If the total, G, is $G \geq 60$ forecast $A_p \geq 100$ for the second day following the flare.

4.2 Estimating $A_p$ From $A_k$. The $A_k$ as determined for Fredericksburg, Va. is used as the basis for estimating $A_p$ until $A_p$ values are compiled and published. For low and high values of $A_p$, $A_p$ and $A_k$ for Fredericksburg are nearly the same. Figure 4-1 shows the correlation for medium values.

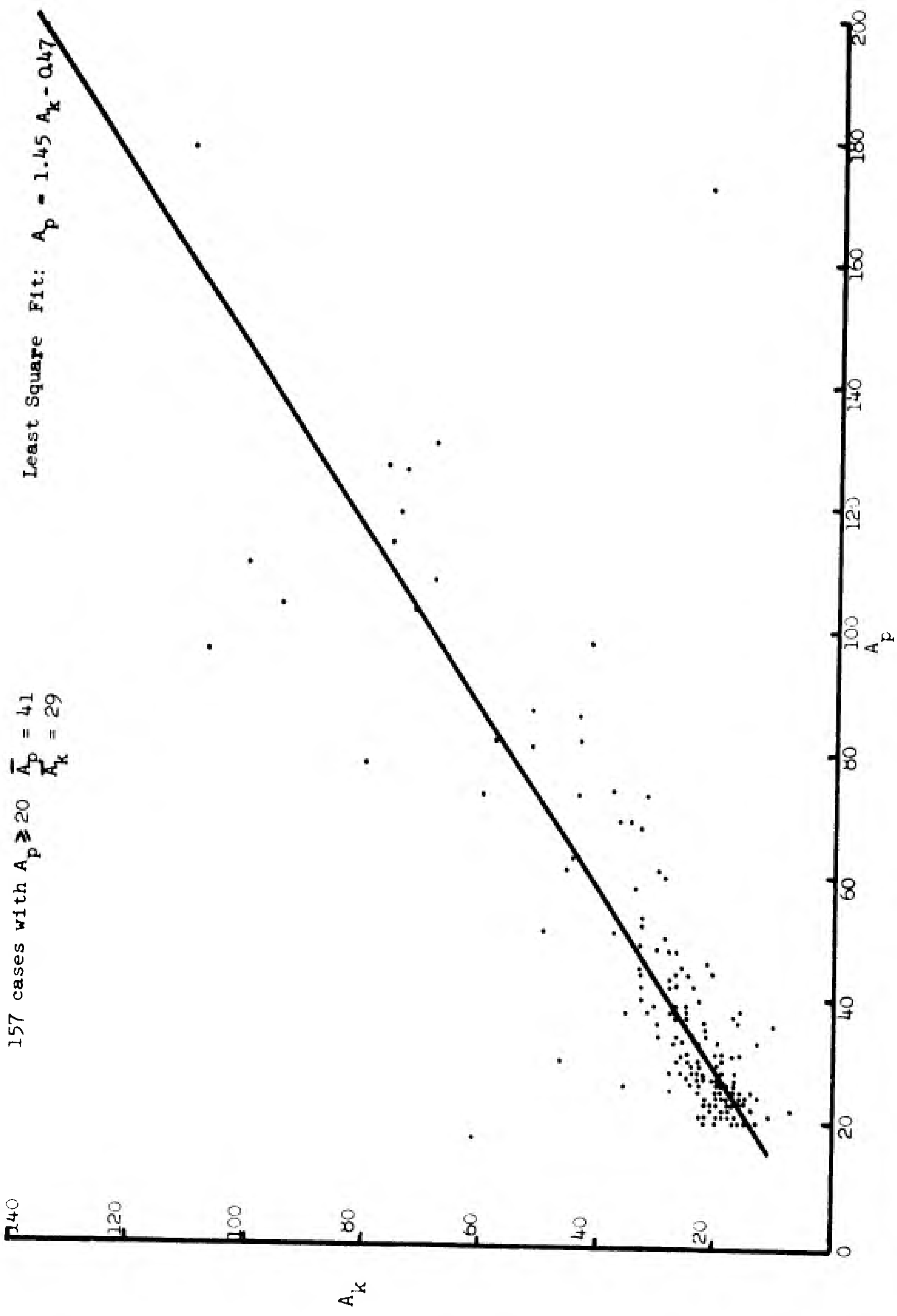


Figure 4-1. Correlation of $A_k$ for Fredericksburg, Va. With $A_p$.

# Chapter 5

## EXTENDED PERIOD FORECASTS

5.1 General. The prediction of most physical parameters over a relatively extended period of time (e.g., in excess of five days) has always been difficult; quite understandably the forecasting of solar activity for such periods is no exception. Comparatively little research has been directed toward methods of extended forecasts of solar parameters, and the product of this limited research has been only partially successful. The Solar Forecast Center, which has been routinely issuing 27-day solar activity forecasts since 13 April 1966, has been attempting to develop and refine forecasting techniques to predict various solar parameters which describe the levels of solar activity over extended periods.

5.2 Philosophy of Extended Period Forecasts. Available research papers on this subject have been screened and portions of many incorporated into forecast procedures at the Center; forecast studies prepared at the Center have proved helpful; several computer programs have been and are being run in a search for additional forecast aids. Given an extant region, its growth and decay patterns may be followed on a day-to-day or shorter time period basis at the SFC. The more active regions usually set up growth patterns which can be extrapolated into the 27-day forecast period. Nevertheless, one very basic problem of solar physics remains unsolved: forecasting the birth of an active region.

5.3 Extended Period Forecast Format and Definitions. A 27-day three-part Extended Period Forecast, with the valid dates given, is issued by the Solar Forecast Center at 1800Z each Tuesday. The valid period and definitions are given in Part I of this forecast. A forecast 27-day mean value of the 2800 MHz flux density is given in Part II with the inclusive dates to expect significant deviations from the forecast mean. The following significant deviation categories are used:

a. MUCH BELOW MEAN. For periods when the daily value is forecast to be more than 20 percent below the expected mean.

b. BELOW MEAN. For periods when the daily value is forecast to be 10 to 20 percent below the expected mean.

c. NEAR MEAN. When the daily value is forecast to be within 10 percent of the expected mean.

d. ABOVE MEAN. For periods when the daily value is forecast to be 10 to 20 percent above the expected mean.

e. MUCH ABOVE MEAN. For periods when the daily value is forecast to be more than 20 percent above the expected mean.

The final portion of the forecast provides an indication of the expected flare activity during the forecast period. A range in the number of importance one, two, three, and four flares which may be expected is given, followed by an appropriate remark indicating the most likely period(s) to expect the most activity.

5.4 Forecast Procedure.

a. Many of the charts, graphs, etc., which are used in making routine daily solar activity forecasts prove useful as aids in preparing extended period forecasts. These include the SFC Active Region History Chart (discussed in 1.4c), a region return list, a record of daily activity, a chart on which the daily 2800 MHz solar radio flux density is plotted, and a chart showing the mean monthly smoothed flux density at 2800 MHz. Additional aids developed by Center personnel and others are also used and are discussed with the above in the following paragraphs.

b. Step One. The first step on the normal forecast procedure involves determining current values and apparent trends of several parameters. The forecaster plots each significant region he expects to be on the visible disk during the 27-day forecast period in a manner similar to that illustrated in Figure 5-1. Historical data are plotted for each region, indicating previous presence of spot groups, 9.1-cm radio-noise sources, flares and significant west-limb tendencies which might have been associated with the previous disk transit. Account is taken of heliographic longitude and latitude and growth/decay patterns the regions have exhibited on their previous passage. As an additional aid, the forecaster employs a set of contingency tables developed by Weddell and Leavell [1963] at North American Aviation. Given the plage parameters of brightness and area, these tables give a percentage probability that a returning plage will produce one or more flares of a certain size during its next transit of the visible disk. The forecaster then assigns a weighting factor (usually on a scale of zero to five) for each region based on both the probability of return and the expectation that such return will exhibit flares and/or spots. These weighted values are then summed over each day

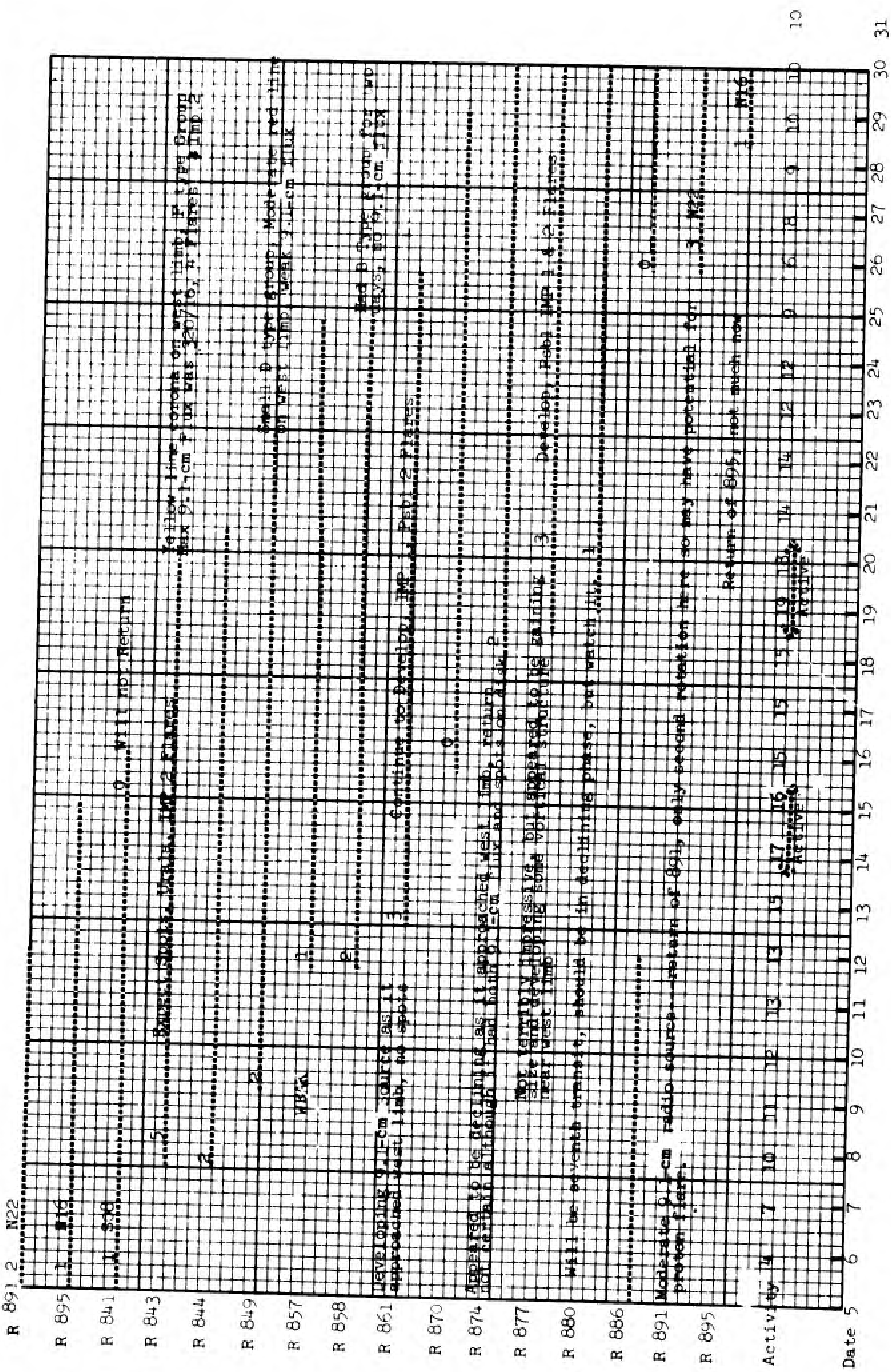


Figure 5-1: Long-Range Forecast Work Sheet

of the forecast interval, thus providing an indication of when various levels of activity are to be expected during the forecast period. Comparison can then be made with previous apparently active longitudes and/or rotation cycles (usually going back only four or so cycles) and appropriate adjustments made. The Solar Forecast Center is presently investigating active longitudes which some researchers [Warwick, 1965] have found to occur, at least insofar as proton producing flares are concerned. There is reason to believe that these longitudes, if they do exist, might well vary from cycle to cycle, and indeed, even within a given cycle. Thus, studies are being conducted at the SFC in an effort to discover which longitudes, if any, seem favorable for the development and growth of plages and sunspots, as well as for those longitudes which seem preferred for flare production. As yet, no positive results have been obtained.

c. Step Two. Step Two involves forecasting the mean 2800 MHz radio flux density (uncorrected to one AU) and significant deviations from this expected mean. A fair first approximation to these parameter may be had by fitting "today's" flux density value to the activity levels obtained in Step One. The forecaster will then consider the expected 27-day running mean for the forecast period. In doing so, he is able to take advantage of the fact that the ascending and descending branches of the solar cycle are relatively linear over a sufficiently long period of time. Cycle 20 has so far proven to be no exception to this tendency and has shown a rather linear increase of flux density over 27-day running mean periods as illustrated by the nomogram in Figure 5-2. The forecaster may extrapolate by straight-line projection an approximate expected mean for the period of his forecast, accurate to within roughly five percent. From experience gained by analysis of Cycle 19, one expects the present slope (about 18% yearly increase) to undergo change. As this change takes place, the forecaster will alter his predictions accordingly. Regression equations developed by The Traveler's Research Center, Inc. for AFCRL are also considered; the preliminary equations listed below predict 27-, 30-, 54-, and 60-day means of radio flux:

(1) Predicted 27-day mean:

$$Y(90) = 4.0210 + 0.38046(Y86) + 0.34343(Y81) + 0.11092(Y13) + 0.12980(Y68)$$

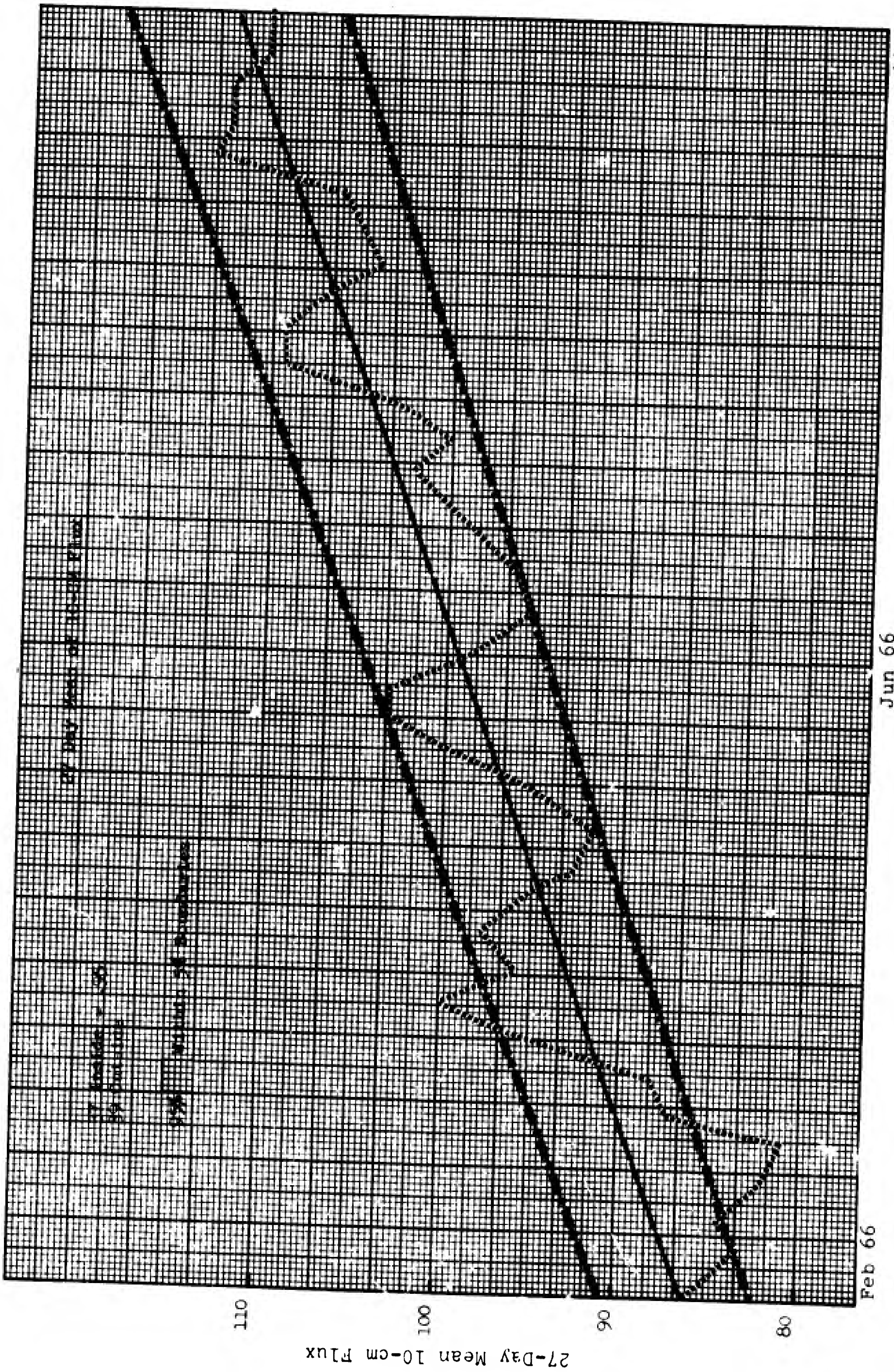


Month

Figure 5-2.

(2) Predicted 30-day mean:

Y(91) = 4.2236 + 0.38821(Y86) + 0.34907(Y81) + 0.11315(Y13) + 0.11246(Y68)

(3) Predicted 54-day mean:

Y(92) = 5.2862 + 0.11777(Y87) + 0.30081(Y81) + 0.079681(Y13) + 0.13815(Y68) + 0.31577(Y89)

(4) Predicted 60-day mean:

Y(93) = 5.5673 + 0.13937(Y87) + 0.29214(Y81) + 0.084741(Y13) + 0.31046(Y89) + 0.12283(Y68)

where

Y(93) = Predicted Mean Flux of Days 1 thru 60

Y(92) = Predicted Mean Flux of Days 1 thru 54

Y(91) = Predicted Mean Flux of Days 1 thru 30

Y(90) = Predicted Mean Flux of Days 1 thru 27

Y(89) = Observed Mean Flux of Days Zero thru -59

Y(87) = Observed Mean Flux of Days Zero thru -29

Y(86) = Observed Mean Flux of Days Zero thru -26

Y(81) = Flux on Day of Forecast (Day 0)

Y(68) = Flux on Day -13

Y(13) = Flux on Day -68

The forecaster then checks the daily solar radio flux density chart for any significant cyclic relationships which have occurred during the past several rotations. Periods of significant deviations from the mean are assigned following the established category definitions. A final check is then made of the preliminary mean value prediction, and any necessary adjustments are made.

d. Step Three. At this point, the forecaster determines the number of flares to be expected in the various importance categories. Three important aids in this procedure are the Active Region History charts (Figure 1-2), a chart relating 2800 MHz flux density and flares (Figure 5-3), and the North American contingency tables [Weddell and Leavell, 1963]. Realistic ranges in the number of flares of each importance are subjectively forecast using these aids.

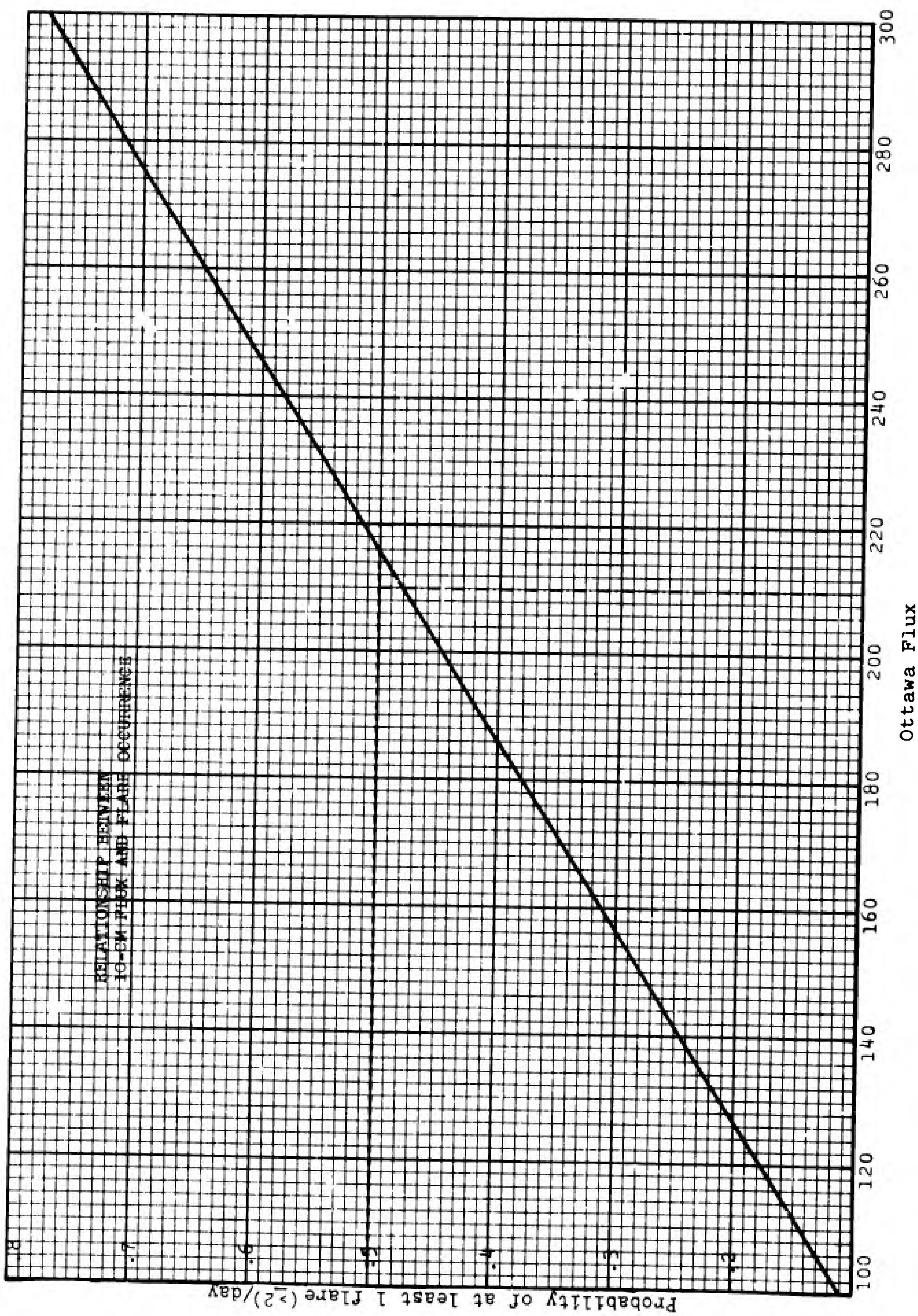
RELATIONSHIP BETWEEN
10-CM FLUX AND FLARE OCCURRENCE
Ottawa Flux
100
120
140
160
180
200
220
240
260
280
300
Probability of at least 1 flare (≥2)/day
.2
.3
.4
.5
.6
.7
.8

Figure 5-3.

e. Step Four. The first three steps involve making the forecast, whereas the final step involves checking the product for consistency. No additional tools are employed; rather each part of the forecast is checked against the others to insure consistency. The flux density forecast is also checked to insure the significant deviation categories are approximately in balance.

5.5 Future of Extended Range Forecasts. It would be incorrect to say there is no skill involved in the preparation and production of extended period solar activity forecasts. Experience at the Solar Forecast Center indicates such a forecast is possible and demand indicates the product is desirable. The problems which confront an extended period forecaster are quite similar (though more massive) to those encountered by forecasters predicting solar activity on a day-to-day basis, namely, development of existing regions, growth and development of new regions, and probability of flare production in these regions. In addition to the programs in progress at the SFC to investigate the possibility of active longitudes, existing data are being re-screened for new predictors other than intensity and brightness of plage areas which might aid in the prediction of birth or return and development of centers of activity. As forecasters gain more experience in handling these complex problems, and with the influx of new data such as daily x-ray measurements, magnetic observations and in-depth measurements of solar radio flux, the Center hopes to develop new tools and techniques which will better enable the forecaster to attack the problems presently confronting him.

**RICHARD M GILL, Colonel, USAF**
**Commander**

OFFICIAL

**WILLIAM [illegible], 2d Lt, USAF**
**Chief, Administrative Services**

## SOLAR FORECAST CENTER STUDIES

A-1. General. Personnel at the Solar Forecast Center are constantly examining both historical and real-time solar data in an effort to develop new forecast techniques and to improve and refine old techniques. The results of a few of these analyses and studies are presented below.

A-2. Spot-Area/Flare Relationship. Figure A-1 represents a part of a continuing data analysis being performed by TSgt Richard Agee. The probability of the occurrence of a flare of Importance Two or greater was determined as a function of spot area for spot groups observed within 60° of the heliographic Central Meridian. Other predictors under study include spot growth rate, age, Zurich (Brunner) class, magnetic class; plage area, brightness, and age; radio brightness at 9.1 cm and 3.4 mm. These studies are particularly valuable because they are based on current data and hence enable forecasters to keep abreast of changing relationships in different stages of the solar cycle.

A-3. Radio Data. Figures A-2 and A-3 were designed to give the forecaster or the forecast user a graphic guide to the character of variations in solar 10-cm radio flux. Figure A-2 should be especially useful to the person interested in a long-range outlook for the expected behavior of solar radio flux in Cycle 20; various horizontal lines on the chart indicate flux values below which the specified percentage of daily readings were observed.

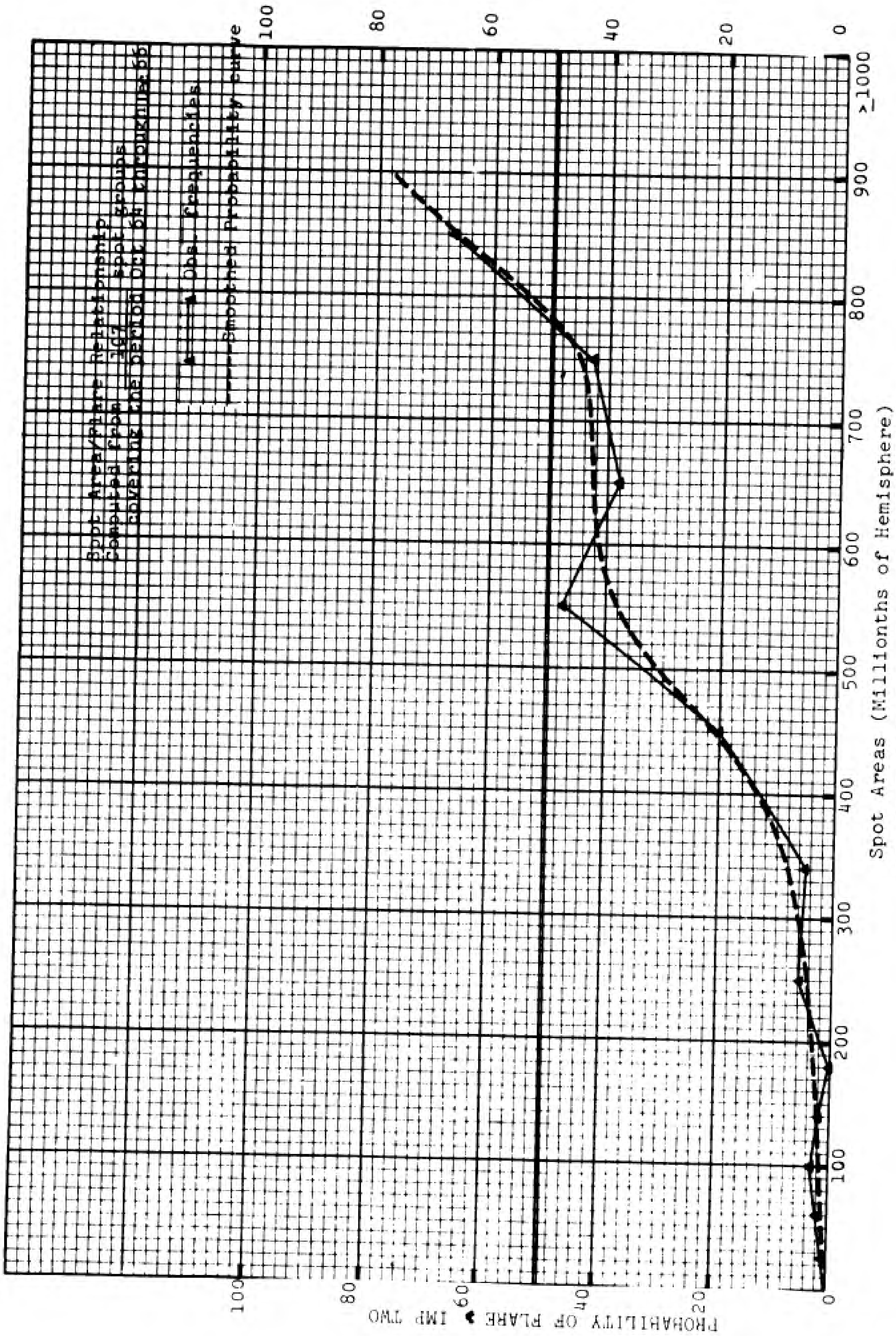
Spot Area/Flare Relationship
Obs. frequencies
Smoothed Probability Curve
100
80
60
40
20
0
≥1000
900
800
700
600
500
400
300
200
100
PROBABILITY OF FLARE ≥ IMP TWO
Spot Areas (Millionths of Hemisphere)
for Spot Locations From 60°E To 60°W

Figure A-1

RANGE OF OBSERVATIONS WITH CERTAIN VALUES OF CORRECTED 2800 MHZ FLUX (BY YEAR)

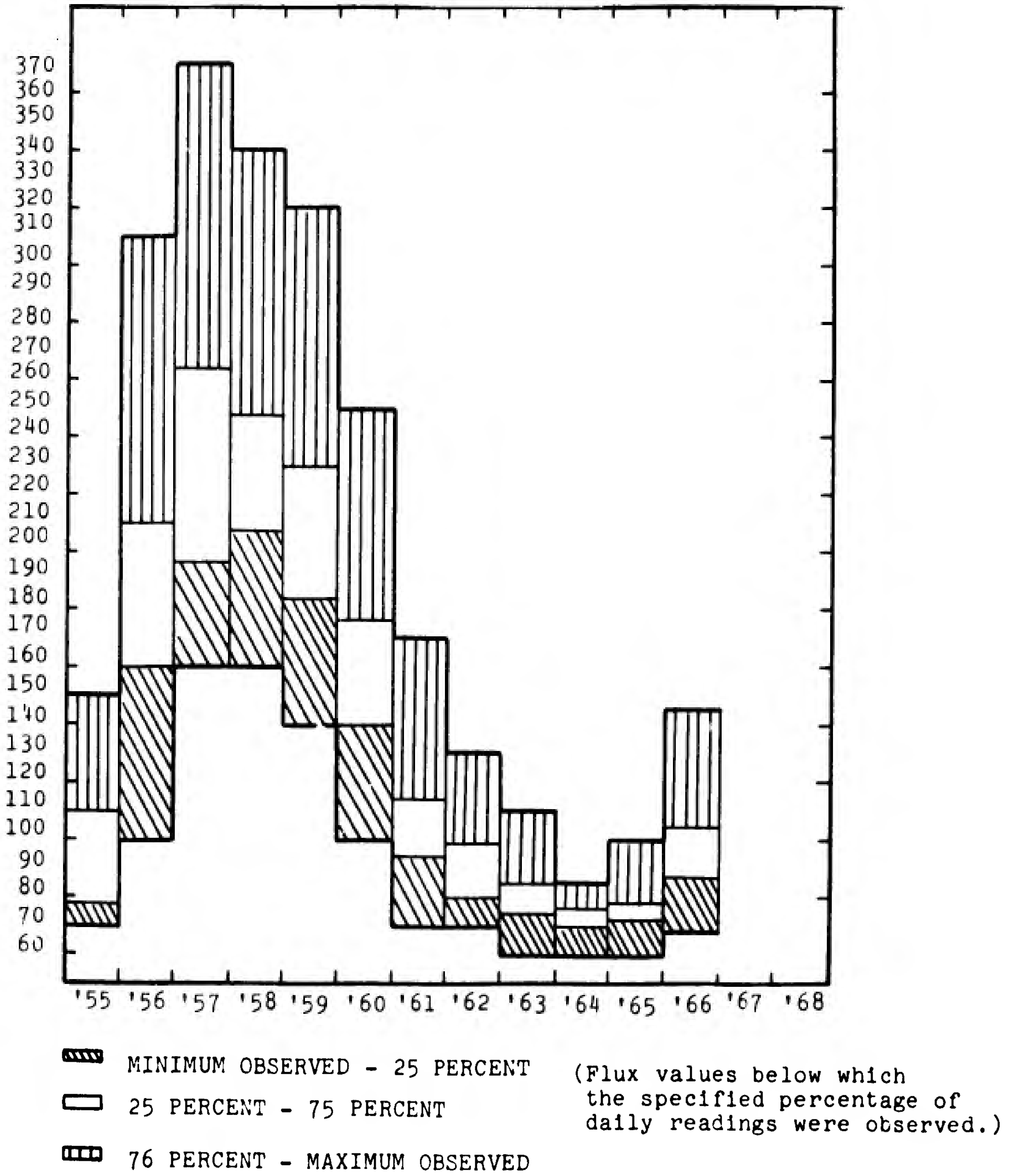


Figure A-2

THE MONTHLY VARIATION OF 2800 MHZ SOLAR FLUX (OTTAWA) FOR THE PERIOD FEBRUARY 1947 - JANUARY 1965 WHICH INCLUDES TWO SOLAR MAXIMUM AND MINIMUM PERIODS.

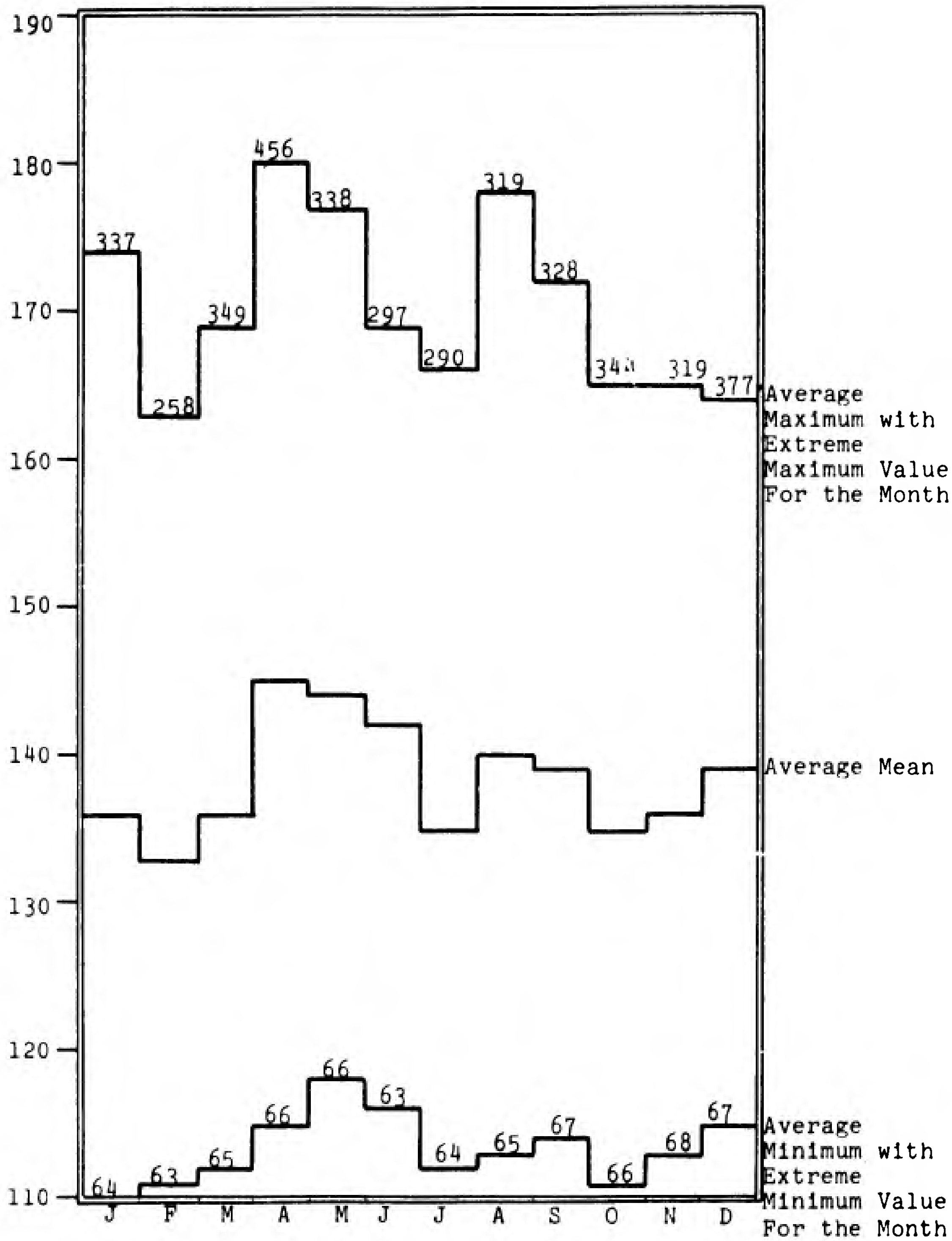


Figure A-3

GEOMAGNETISM

B.1 The Solar-Geomagnetic Relationship. The earth's observed magnetic field is modulated by the interaction of the field with the electromagnetic and corpuscular radiation from the sun.

a. The Earth's Main Magnetic Field. The earth's main magnetic field is the part of the observed field that originates in the interior of the planet. This main field is to a first approximation a dipole magnetic field. Most of the main field is believed to arise from electric currents that flow in the molten metallic core of the earth. While the configuration of the internal currents is such that the field at the surface resembles that of a dipole, there are regional and surface anomalies which cause significant departures from a dipole field over large areas of the earth. The magnetic field is a vector-field. That is, the earth's magnetic field at every point has both a magnitude and a direction. The three basic elements of the magnetic field vector, $\vec{F}$, are the horizontal plane component, $\vec{H}$, the declination angle, D, and the inclination angle or dip angle, I. These basic elements are shown in Figure B-1.

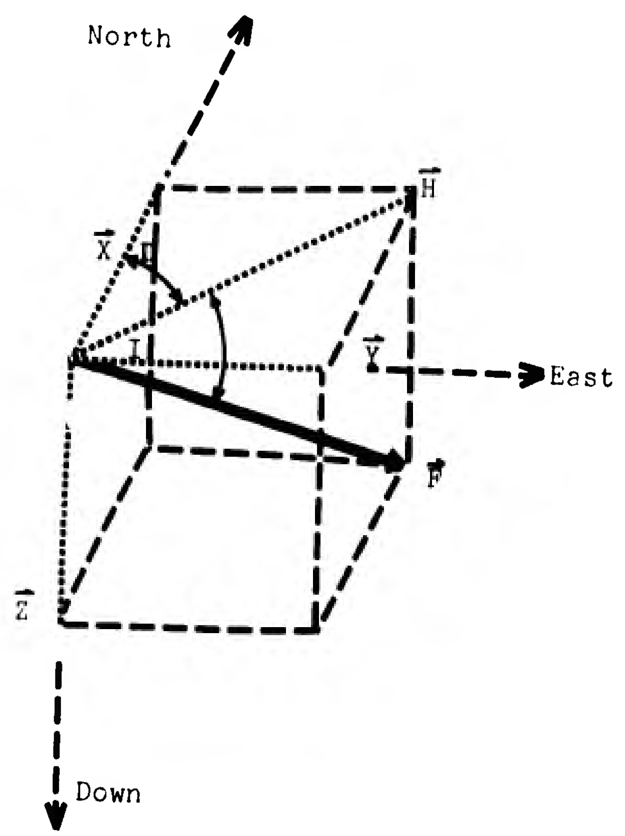


D = Angle between $\vec{X}$ and $\vec{H}$

I = Angle between $\vec{H}$ and $\vec{F}$

Figure B-1. Elements of the Magnetic Field Vector F

The magnetic field vector can be described by other combinations of three elements such as $(\vec{X},\vec{Y},\vec{Z})$, $(\vec{H},D,\vec{Z})$ or $(|\vec{F}|, I, D)$. $\vec{X},\vec{Y},\vec{Z}$ are the three local conventional cartesian components of the magnetic field vector $\vec{F}$. The sign conventions for the magnetic field elements are as follows:

$\vec{X}$ = Positive North.

$\vec{Y}$ = Positive East.

$\vec{Z}$ = Positive to the nadir (down).

D = Positive measured Eastward from North in the horizontal plane.

I = Positive measured downward from $\vec{H}$ to $\vec{F}$ in the vertical plane.

The $\vec{X},\vec{Y},\vec{Z}$ and $\vec{H}$ components as well as the magnetic field vector $\vec{F}$ are measured in gauss ($\Gamma$) or gammas ($\gamma$). One hundred thousand $\gamma$'s are equal to one gauss. ($\Gamma = 10^5\gamma$). The magnetic field at the surface of the earth varies from approximately 0.6 gauss in the polar regions to about 0.3 gauss in the equatorial regions.

b. The Magnetosphere and the Relationship to the Solar Wind. With the advent of satellites we have the ability to investigate the magnetic fields that surround the earth. At the same time interest developed in the continual corpuscular radiation from the sun. From the satellite observations a rather comprehensive but qualitative picture has developed for the general interaction of the solar wind and the magnetic field of the earth. Corpuscular radiation is continually emitted from the sun in the form of a plasma. The energy density of the flowing plasma from the sun (solar wind) is great enough to confine the magnetic field of the earth to the general configuration shown in Figure B-2.

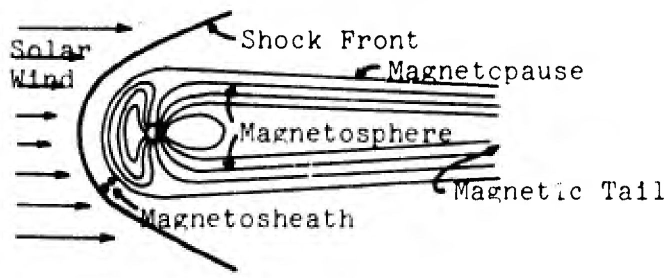


Figure B-2. Schematic of Geomagnetic Field

Little is known about the exact shape of the geomagnetic tail; however, it is felt that the tail extends beyond the orbit of the moon. Changes in the flux of the solar wind cause changes in the configuration of the magnetosphere and the associated boundary surfaces. As the configuration of the magnetosphere changes so does the magnetic field at the surface of the earth.

c. The Earth's Ionosphere, Solar Electromagnetic Radiations, and Their Relation to Geomagnetism. A current flow will produce an associated magnetic field. Several variations in the geomagnetic field are caused by transient currents that flow in the earth's ionosphere. A current flow requires charged particles. Electromagnetic radiation of less than 3000 Å is absorbed by the atmosphere constituents. The energy of the radiation between 1000 - 3000 Å is not great enough, except for the Lyman-alpha radiation of hydrogen near 1216 Å, to photoionize the atmospheric constituents. The solar radiation of less than 1000 Å is primarily responsible for the formation of charged particles in the ionospheric regions of the earth's atmosphere. The solar radiation of less than eight Angstroms is responsible for the ionospheric D layer. During a solar flare this x-ray radiation is greatly enhanced. The combination of the ionizing electromagnetic radiations from the sun, the earth's magnetic field, the heating of atmosphere by the sun, the lunar and solar tidal forces, and the electrostatic forces all add to produce ionospheric currents which are responsible for many variations of the geomagnetic field that are observed at the surface of the earth.

d. Solar Flares and Their Relation to Geomagnetism. During a solar flare the extreme ends of the electromagnetic radiation spectrum are greatly enhanced. Corpuscular radiation, which may be considered as extremely high frequency electromagnetic radiation, is included in the flare enhancement of radiation. A crochet is the geomagnetic record of the solar flare enhancement of x-rays. The solar corpuscular radiation from the flare travels on the order of a 1000 km/sec. This implies a time delay of about 2 days before the corpuscular radiation reaches the earth. A shock front precedes the plasma cloud as the cloud travels to the earth. The traveling shock wave interacts with the standing shock front of the magnetosphere, and this produces a compression of the magnetosphere. This compression is observed at the earth's surface as a sudden increase in the H component. This sudden increase is referred to as a sudden commencement and the increase is followed by a geomagnetic storm. A geomagnetic storm has different characteristic magnetogram traces at different geomagnetic latitudes. This fact is depicted in Figure B-3 [Hines, Paghis, Hartz, and Fejer, 1965].

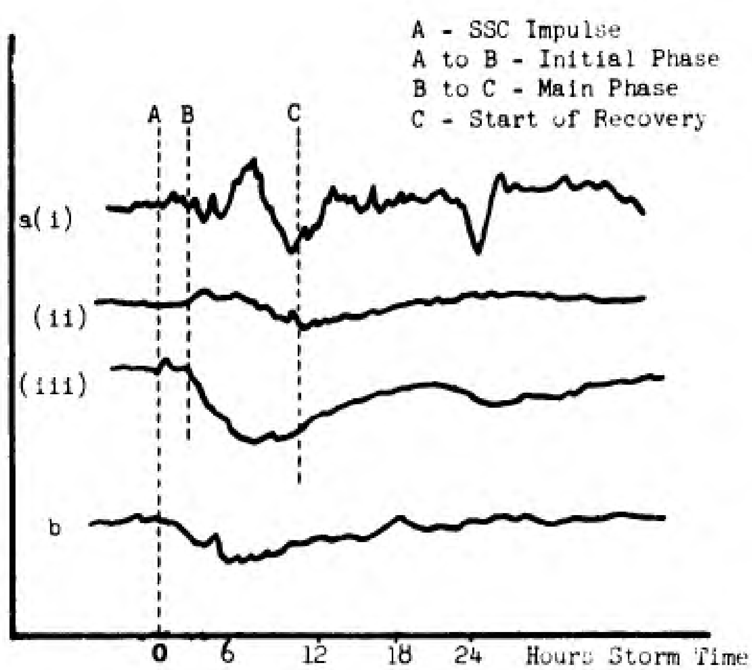


Figure B-3. Variations in the Horizontal H Component of Standard Magnetograms During Storms.

(a) SC (Sudden Commencement) Storm

(i) In the polar cap.

(ii) Near the auroral zone (vertical scale is reduced by a factor of ten).

(iii) At low latitude.

(b) GC (Gradual Commencement) Storm at Low Latitude

The classical magnetogram record of a geomagnetic storm is that of the low latitude station. The initial phase is explained by the compression of the magnetosphere. The main phase decrease in the magnitude of the H component at low latitudes is usually explained by the energizing of an equatorial east-to-west ring current. The energizing of the ring current is thought to be related to the plasma cloud which follows the traveling shock front. The decay of the ring current corresponds to the recovery phase of the geomagnetic storm at low latitudes.

B.2 The Geomagnetic Indices K, $A_k$ and $A_p$. K, $A_k$, and $A_p$ are geomagnetic indices which reflect the irregular variations in magnetograms. The K index is the basic index from which the $A_k$ and $A_p$ indices are derived. These three indices reflect the geomagnetic variations which are caused by the variability in the solar corpuscular radiation and the corpuscular radiation's interaction with the earth's magnetosphere.

a. The K Index. The K index evaluates disturbed geomagnetic activity during each three-hour interval of the Greenwich day. During periods of low solar activity (quiet sun) there are regular diurnal geomagnetic variations which are repetitive and predictable. These are the solar quiet day variations ($S_q$) and the lunar variations (L). The K index must not reflect these variations. The K index reflects the maximum three-hourly range in X,Y or Z components after the expected $S_q$ and L variations have been accounted for in the magnetometer trace of each of the three components. For middle latitude stations, such as Fredricksburg, the K index of 0 to 9 corresponds to the following ranges in the corrected H component variations measured in $\gamma$'s.

| $K_p$ | 0 | 1 | 2 | 3 | 4 |
|---|---|---|---|---|---|
| $\gamma$ range | 0 to 5 | 5 to 10 | 10 to 20 | 20 to 40 | 40 to 70 |

| $K_p$ | 5 | 6 | 7 | 8 | 9 |
|---|---|---|---|---|---|
| $\gamma$ range | 70 to 120 | 120 to 200 | 200 to 320 | 320 to 500 | >500 |

In polar latitudes the H component is normally small, but the polar latitude H component has greater variations than the variations in the normally large H component of the equatorial latitudes. For this reason the $\gamma$ range for the K index must vary with latitude in order that the K indices should correspond reasonably well from station-to-station. The $\gamma$ range chosen for the various observatories indicates the latitude variation in geomagnetic activity. In low latitudes a K index of 9 represents a $\gamma$ range of at least 300; whereas in the auroral zone a K index of 9 may represent a $\gamma$ range of 2500 or more.

b. The $A_k$ Index. Once the K index values are known, it is a simple conversion to the $a_k$ three-hourly index values. The conversion is as follows:

| $K_p$ | 0 | 1 | 2 | 3 | 4 | 5 | 6 | 7 | 8 | 9 |
|---|---|---|---|---|---|---|---|---|---|---|
| $a_k$ | 0 | 3 | 7 | 15 | 27 | 48 | 80 | 140 | 240 | 400 |

The K index is a semi-logarithmic scale, and the $a_k$ index is an attempt to unwind the logarithmic scale into a linear scale such that a daily average of the eight $a_k$ values is a meaningful geomagnetic activity indicator. The following will serve as an example of the trouble in taking daily averages of the eight K indices. Suppose that the following arbitrary K index records are for two arbitrary days:

K 1 1 1 1 1 1 1 1 Day 1

K 0 0 0 0 0 0 0 8 Day 2.

An average of the eight K indices would yield the same result for each day; however, the second day is far more disturbed geomagnetically than the first day of the arbitrary example in which the K index is one for each three-hour period. To convert the K indices to a single daily $A_k$ index, which is the arithmetic average of the eight three-hourly $a_k$ indices, alleviates the problem partially. In the example given above, the first day $A_k$ would be three and the second day $A_k$ would be 30. The value of 30 reflects the abnormally large geomagnetic disturbance that occurred at the end of day 2.

c. The $A_p$ Index. The $A_p$ index is reduced from the K indices from 12 geomagnetic observatories. Eleven of these observatories are in the northern hemisphere and the twelfth observatory is in New Zealand. The K indices from each of the 12 observatories are reduced to eliminate local time and seasonal effects. The result is a standardized index $K_s$ for each station on a scale from 0o to 9o. The average of the 12 $K_s$ indices is the planetary $K_p$ index for each three-hour period. The $K_p$ index is converted to a linear scale $a_p$ by the following conversion table:

| | | | | | | | | | | | | |
|---|---|---|---|---|---|---|---|---|---|---|---|---|
| $K_p$ | 0o | 0+ | 1- | 1o | 1+ | 2- | 2o | 2+ | 3- | 3o | 3+ | 4- |
| $a_p$ | 0 | 2 | 3 | 4 | 5 | 6 | 7 | 9 | 12 | 15 | 18 | 22 |
| $K_p$ | 4o | 4+ | 5- | 5o | 5+ | 6- | 6o | 6+ | 7- | 7o | 7+ | 8- |
| $a_p$ | 27 | 32 | 39 | 48 | 56 | 67 | 80 | 94 | 111 | 132 | 154 | 179 |
| $K_p$ | 8o | 8+ | 9- | 9o | | | | | | | | |
| $a_p$ | 207 | 236 | 300 | 400 | | | | | | | | |

The average of the eight $a_p$ values for each Greenwich day is the equivalent daily planetary amplitude index $A_p$.

## GLOSSARY

Abbreviations: The following abbreviations are frequently used in the forecast messages issued by the Solar Forecast Center. They are discussed in the definitions below:

| | |
|---|---|
| $A_k$, $A_p$ | Geomagnetic indices |
| APR | Active Prominence Region |
| B | Brilliant Flare |
| BSD | Bright Surge on Disk |
| F | Faint Flare |
| IMP | Importance |
| N | Normal Flare |
| PCA | Polar Cap Absorption |
| R | Sunspot Number |
| SC | Sudden Commencement |
| SCNA | Sudden Cosmic Noise Absorption |
| SEA | Sudden Enhancement of Atmospherics |
| SFD | Sudden Frequency Deviation |
| SID | Sudden Ionospheric Disturbance |
| SPA | Sudden Phase Anomaly |
| SWF | Short Wave Fade-out |

Active region: A region on the sun which has the potential to produce a flare or has already produced a flare. The region will normally be a radio noise source, have a moderately large and bright plage, and contain a sunspot group.

$A_k$, $A_p$: $A_k$ is a local geomagnetic index representing the degree of geomagnetic variability for one station for one day. Variability is reported by a "K" index at the end of each three-hour period during the day; the eight K figures (ranging from 0 to 9) are converted to eight "a" indices (ranging from 0 to 400) which are averaged over a day to derive the value for $A_k$. In general $A_k$ values increase toward the poles. $A_p$ is the planetary average of $A_k$ values for 12 selected stations for one day.

Angstrom: Unit of length equal to $10^{-8}$ cm. The wavelengths of spectral lines are usually given in angstrom units (Å).

Aurora: The sporadic radiant emission from the upper atmosphere over middle and high latitudes. It is believed that charged particles (electrons and, to a lesser extent, protons) interacting with the earth's magnetic field and atmosphere excite the atmospheric gases which then emit visible radiation. The aurora is most intense at times of magnetic storms, when it is also observed farthest equatorward. The distribution with height shows a pronounced maximum near 100 km. The lower limit is probably near 80 km.

Brunner (or Zurich) Sunspot Classification: A sunspot group can be classified into nine types according to its stage of growth development or decay. These types, A through J, are described below:

A. Composed of a small single spot or a very small group of spots, mostly of short durations, concentrated in a region of 2-3 square degrees. No systematic structure of the group; spots without penumbra.

B. Bipolar group of spots without penumbra, the long axis of which is directed roughly east-west. Concentration of spots on east and west ends.

C. Bipolar group like B, but at least one main spot with penumbra.

D. Bipolar group, the main spots showing penumbrae. At least one of two main spots simple. Longitude greater than $10^{\circ}$.

E. Large bipolar group showing a complicated structure, the two major spots each having a penumbra. Numerous small spots between the major spots. Dimension of the group in longitude at least $10^{\circ}$.

F. Very large bipolar or complex group. Dimension in longitude at least $15^{\circ}$.

G. Large bipolar group, without small spots between the two major spots. Dimension in longitude at least $10^{\circ}$.

H. Unipolar spot with penumbra. Sometimes with complicated structure. Diameter greater than $2.5^{\circ}$.

J. Unipolar spot with penumbra. Round shape, diameter less than $2.5^{\circ}$.

Central Meridian: An imaginary line, connecting the solar rotational poles, running through the center of the disk as seen from the earth. The locations of solar features are referred to this line (CMD: Central Meridian Distance, in degrees E or W) and to the solar rotational equator (latitude, in degrees N or S).

Chromosphere: The layer of the sun immediately above the photosphere. The chromosphere is not visible to the naked eye because, even though it is hotter than the photosphere, it is very tenuous. Many important phenomena occur in the chromosphere, e.g., flares.

Corona: The very low density layer or envelope just above the chromosphere. It is hotter and even more tenuous than the chromosphere and can be studied only during an eclipse, either man-made or natural. Low frequency radio noise has its origin in the corona. Coronal temperatures exceed $10^6$ degrees with local hot spots of 4-5 times $10^6$. The corona can be studied through its emission in several spectral lines. The red line (6374 Å) and green line (5303 Å) are the two most commonly observed lines. When the corona is highly disturbed it is possible to detect a yellow line (5694 Å).

Cosmic Rays: High-energy particles, usually from galactic sources, which are received continuously at the earth. Secondary radiation produced in the upper atmosphere can be detected at the earth's surface by neutron monitors. Galactic cosmic rays are modulated by solar activity; after a major solar flare there is often a decrease in the level of cosmic ray reception (Forbush decrease). A few of the more intense solar flares produce particles of sufficient energy to be called solar cosmic rays; in these instances, counting rates of detectors on the earth's surface are observed to rise.

Electron Density: $n_e$ is the number of free electrons per unit volume. This is the parameter that is most important in determining the characteristics of the ionosphere. It is also an indicator of solar activity. Short wave and particulate solar radiation produce free electrons by ionization of the molecules and atoms in the earth's atmosphere.

Electron Volt: One ev is the amount of energy acquired by an electron which has passed through a potential of one volt.

1 ev = $1.60 \times 10^{-12}$ ergs
1 Kev = $10^3$ ev
1 Mev = $10^6$ ev
1 Gev = $10^9$ ev

Filament: See Prominence.

Flare: A transient, localized brightening of the chromosphere; generally associated with a plage. Flares are usually observed at the wave length of H alpha (6563 Å). Emission at almost all wave lengths, from the very short x-rays to the longer radio waves, is enhanced. Corpuscular radiation is often increased. Flares are classified into five main categories with three sub-categories, faint (F), normal (N), or brilliant (B). The main importance categories 0, 1, 2, 3, and 4, are based solely on the corrected area (millionths of solar hemisphere) of the flare at the time of maximum intensity. Thus a flare will have any one of 15 classifications, importance OF to 4B. The table below gives the characteristics of the main categories:

| Class | Average Duration (minutes) | Area (millionths of Solar Hemisphere) | Frequency of Occurence (Pct) |
|---|---|---|---|
| 0 (F, N, & B) | 17 | less than 100 | 75.0 |
| 1 (F, N, & B) | 32 | 100 to 249 | 19.6 |
| 2 (F, N, & B) | 69 | 250 to 599 | 4.8 |
| 3 (F, N, & B) | 145 | 600 to 1200 | less than 1 |
| 4 (F, N, & B) | 145 | more than 1200 | less than 1 |

Geomagnetic Storm:

a. Recurrent storms are storms which recur in a 27-day cycle. They may not be related to a visible solar region but are related to the so-called M-regions on the sun. They are caused by low energy solar particles of the order of 400 ev.

b. Sudden commencement (SC) storms begin more suddenly than recurrent storms and usually reach higher $A_p$ values. The particles causing these storms are in the 10 Kev energy range. Some fairly large flares are followed within about 20 to 60 hours by a SC.

H-Alpha: A particlar spectral line, normally an absorption feature in the red end of the solar spectrum (6563 Å) in which most solar activity is observed optically. In major flares H-alpha may be observed in emission rather than absorption. H-alpha is the first Balmer line for the hydrogen atom.

Ionosphere: The region in the upper atmosphere (80-400 or more km) in which solar radiation produces a rather large electron density ($n_e = 10^4 - 10^6 cm^{-3}$). The ionosphere is vital to radio communications because it is used with the earth's surface to form a "duct" for certain radio waves; for certain radio frequencies the ionosphere is used to "bounce" or to reflect radio signals from one surface station to another. Changes in the ionosphere produced by solar influences can disturb or even completely destroy radio communication links. Observations of ionsopheric disturbances may be used to infer the occurrence of solar events such as flares.

Limb: The apparent edge of the sun.

M-region: A hypothetical particle-emitting region on the sun. M-regions apparently recur every 27 days since they produce recurrent magnetic storms of that periodicity. However, they have never been identified by optical observations.

Magnetic Classification of Sunspots:

ALPHA: (unipolar) A spot or group of spots with a single magnetic polarity.

BETA: (bipolar) A group of spots having opposite magnetic polarities in the preceding and following parts.

BETA-GAMMA: A group of spots having bipolar characteristics but with no marked N-S dividing line between the spots of different polarities.

GAMMA: A complex group with spots of both polarities irregularly distributed.

DELTA: Spots of opposite polarity separated by not more than two degrees within the same penumbra.

Neutron Monitor: A device which counts the number of neutrons received at the earth's surface. It provides an indirect count of cosmic rays, since the primary cosmic rays create secondary neutron emission after encountering air molecules or atoms.

Photosphere: The surface of the sun as seen by the naked eye. The photosphere appears white, except for the sunspots which are dark.

**Plage**: A cloud of ionized gas in the chromosphere. Plages are not visible to the naked eye. They are studied by means of telescopes equipped with monochromatic filters.

Polar Cap Absorption (PCA): An ionospheric phenomenon evidenced by enhanced absorption of radio waves in the polar regions. Absorption of radio noise from galactic sources is observed with a RIOMETER (Relative Ionospheric Opacity Meter); absorption of terrestrial waves is observed by VHF forward scatter and partial reflection techniques. A PCA is used to verify the "proton event" forecast issued by the Solar Forecast Center.

Polar Cap Event (PCE): A general term describing the ionization caused by precipatating solar particles and the associated effects (both absorption and enhancement) on radio waves. This term includes all PCA's.

Prominence: A formation of hydrogen and other ionized gases, sometimes in the form of loops or arches, seen at the limbs. Quiescent prominences are the more stable type. When seen against the disk they are called filaments and have dark sinuous forms. They maintain their form for many days at a time. Active region prominences and filaments are less stable and may disappear from view. Thus a sudden disappearance of a filament (SDF) may be evidence of proton emission. The abbreviation for an active prominence region is APR.

Proton Event: The detection at the earth of a sudden increase in the number of solar protons of energy greater than 20Mev. Detection may be accomplished directly by satellite or may be inferred from various observations of perturbations of the ionosphere. (See "Polar Cap Absorption").

Proton Flare: A flare which produces energetic particles subsequently observed at the earth as a Polar Cap Event.

Proton Plage: A plage from which energetic particles have been ejected, resulting in a PCE.

Radio Bursts: Sudden increases in flux at various radio wavelengths. Meter-wavelength events are classified as follows:

Type I: Radio noise storms consisting of enhanced continuum radiation and series of short bursts, often several hundred per hour, occurring over wide frequency ranges.

Type II: Slow-drift bursts caused by a source moving outwards through the corona at a relatively low velocity (1000-1500 km/sec). The frequency of emission enhancement decreases slowly (hence the name, "slow-drift").

Type III: Fast-drift bursts caused by a source moving at one-half to one-third the speed of light upwards through the corona. Emission frequency decreases rapidly.

Type IV: Broad band continuum emission (occasionally extending into the centimeter wavelengths) emanating from a source of large extent that moves outward to heights of the order of a solar radius, typically persisting for tens of minutes and sometimes lasting for several hours. Type IV bursts often follow Type II bursts and are considered to be good evidence for proton emission.

Type V. Wide-band continuum emission similar to Type IV except that it is associated with Type III bursts rather than Type II, has a shorter lifetime, and is usually observed only at the lower frequencies.

Centimeter-wavelength bursts are normally observed at single frequencies, although they appear to have a broad-band continuous spectrum. Most bursts exhibit a simple rise in intensity followed by a gradual decay; bursts may be classified into three basic types which may occur in combination to produce any given event:

Type A: Simple Burst. Characterized by impulsive, rapid rise and short duration (normally 1 to 5 minutes); simple bursts may occur in series or in groups and will then be identified as "complex" bursts.

Type B: Post-burst. Follows a simple burst or group of simple bursts and lasts several minutes to several hours; appears as a very slow decay of the Type A burst.

Type C: Gradual rise and fall. Characterized by a slow rise to peak intensity and a slower decay; lasts 10 minutes or longer.

Radio Flux: Flux, in general, is the rate of flow of some quantity, often used in reference to the flow of some form of energy. Flux density is the flux of any quantity through a unit area of specified surface (in the case of radio flux, the unit area is one square meter at the top of the earth's atmosphere). The radio flux density at 2800MHz (10.7 cm) is a useful indicator of solar activity; it exhibits both 11-year and 27-day periodicities. It is measured daily at several observatories, but the standard data source is Ottawa, Canada. The units are $10^{-22}$ watts/square meter/cycle per second bandwidth.

Sudden Ionospheric Disturbance (SID): A sudden ionospheric response that correlates best with centimeter solar radio bursts. SIDs are caused by either an enhancement of ionization or by the formation of a new region in the lower ionosphere. Several types are recognized:

SCNA: A sudden cosmic noise absorption is similar to PCA but lasts typically for minutes or hours rather than days. It is caused by increased electron density in the lower ionosphere which increases absorption of cosmic noise, particularly around 18-30 MHz. It is one of the best indirect indicators of flare activity.

SEA: A sudden enhancement of atmospherics is an increase in the low frequency atmospherics signal (e.g., thunderstorms at around 30KHz) due to an increase in ionospheric reflectivity.

SPA: A sudden phase anomaly occurs when the base of the ionosphere is suddenly lowered, thus changing phase differences between sky radio waves and ground radio waves.

SWF: A short wave fade-out is a decrease in signal strength of 5-20 MHz radio waves transmitted by ground stations caused by increased absorption in the lower ionosphere.

Sunspots: Sunspots are dark, relatively cool areas on the photosphere which act as foci for solar active regions; they are thought to be caused by the inhibition of the convective transfer of energy resulting from the presence of strong magnetic fields. The larger and fast growing sunspots are often associated with large flares. Size, rate of growth, decay and magnetic complexity are important in determining the chances of flares.

Sunspot Cycle: The general level of solar activity exhibits an average periodicity of about 11 years. Past cycles have been as short as seven years and as long as 17 years. One of the parameters used to establish this periodicity has been the sunspot number. The maximum of the last cycle (cycle 19) was in March 1958; the last minimum was in October 1964. The next maximum (cycle 20) is expected late in 1968 or in 1969.

Sunspot Number: A solar index which has been compiled back to about 1600 A.D. Although other indices may be more objective, the sunspot number is very useful because of the long period of record. The sunspot number takes into account the number of sunspot groups as well as the number of individual spots.

$$R = K (10g + s)$$

where R = sunspot number

g = number of groups

s = number of spots

k = a constant, roughly equal to 1, used to adjust individual R numbers to account for some observatories having better observing conditions than others.

THIS IS A BLANK PAGE

## BIBLIOGRAPHY OF MATERIAL REFERENCES


1. Bartels, Julius, 1934, "Twenty-seven Day Recurrences in Terrestrial-Magnetic and Solar Activity, 1922-33." Terrestrial Magnetism, Vol. 39, 201-2.

2. Bell, Barbara, 1961, "Major Flares and Geomagnetic Activity." Smithsonian Contributions to Astrophysics, Vol. 5, No. 7, 69-83.

3. Bell, Barbara and Richard J. Defouw, 1966, "Dependence of Lunar Modulation of Geomagnetic Activity on the Celestial Longitude of the Moon." Journal of Geophysical Research, Vol. 71, 951-957.

4. Bell, Barbara and Richard J. Defouw, 1966, "On the Lunar Modulation of Geomagnetic Activity, 1884-1931 and 1932-1959." Journal of Geophysical Research, Vol. 71, 4599-5603.

5. Bigg, E. K., 1963, "Lunar and Planetary Influences on Geomagnetic Disturbances." Journal of Geophysical Research, Vol. 68, 4099-4104.

6. Bigg, E. K., 1964, "Lunar Influences on the Frequency of Magnetic Storms." Journal of Geophysical Research, Vol. 69, 4971-4974.

7. Bowen, E. G., 1964, "Lunar and Planetary Tails in the Solar Wind." Journal of Geophysical Research, Vol. 69, 4969-4970.

8. Brandt, John C., and Paul W. Hodge, 1964, Solar System Astrophysics. New York: McGraw-Hill Book Company, Inc.

9. Bray, R. J. and R. E. Loughhead, 1965, Sunspots. New York: John Wiley & Sons.

10. Bruzek, A., 1964, "On the Association Between Loop Prominences and Flares." The Astrophysical Journal, Vol. 140, 746-759.

11. Cahill, Laurence J., 1965, "The Magnetosphere." Scientific American, Vol. 212, 58-68.

12. Cole, K. D., 1965, "Stable Auroral Red Arcs, Sinks for Energy of Dst Main Phase." Journal of Geophysical Research, Vol. 70, 1689-1706.

13. Cole, K. D., 1966, "Magnetic Storms and Associated Phenomena." Space Science Review, Vol. 5, 699-770.

14. Chapman, Sydney, and Julius Bartels, 1940, Geomagnetism, (Volumes I and II). London: Oxford University Press.

15. Davidson, T. W. and D. F. Martyn, 1964, "A Supposed Dependence of Geomagnetic Storminess on Lunar Phase." Journal of Geophysical Research, Vol. 69, 3973-3979.

16. Dodson, H. W. and E. R. Hedeman, 1964-66, "Studies of Flares Associated with Cosmic Ray Events." Unpublished Course Notes, McMath-Hulburt Observatory, University of Michigan.

17. Dodson, Helen W. and E. Ruth Hedeman, 1964, "Problems of Differentiation of Flares with Respect to Geophysical Effects." Planetary and Space Science, Vol. 12, 393-418.

18. Dubs, C., R. Filz, L. Katz, D. Smart, A. Weinberg, and K. Yates, "Corpuscular Radiation." Handbook of Geophysics and Space Environments, (S. L. Valley, ed.), Air Force Cambridge Research Laboratories: Office of Aerospace Research, USAF.

19. Enger, I., R. T. Podsiadlo, D. C. Jensen, and F. Ward, 1966, Solar Flare Occurrence as a Function of Sunspot Size. Air Force Surveys in Geophysics, No. 178, Air Force Cambridge Research Laboratories.

20. Gnevyshev, M. N. and L. Kriusky, 1966, "The Relation Between Proton Flares and the Corona Over the 11-year Cycle." Soviet Astronomy, Vol. 10.

21. Harvey, G., 1965, "2800 Mc/s Radiation with Solar Radio Bursts." Journal of Geophysical Research, Vol. 70, 2974.

22. Hess, Wilmont N. (Editor), 1964, AAS-NASA Symposium on the Physics of Solar Flares, Washington D. C.: Scientific and Technical Division, NASA.

23. Hines, C. O., I. Paghis, T. R. Hartz, and J. A. Fejer (Editors), 1965, Physics of the Earth's Upper Atmosphere. Englewood Cliffs, New Jersey: Prentice-Hall Inc.

24. Jonah, Fred C., 1966, Analyses of Polar Cap Absorption Events. Ling-Temco-Vought Report No. 00.802.

25. Jonah, F. C., H. Dodson-Prince, and E. R. Hedeman, 1964-1965, Solar Activity Catalog, Vols. 1-5. National Aeronautics and Space Administration.

26. Lopez, M.D., A. L. Bragg and J. L. Modisette, 1966, "Preliminary Warning Criteria for the Solar Particle Alert Network." NASA Program Apollo Working Paper No. 1193, NASA Manned Spacecraft Center.

27. Maer, Kemp, Jr. and A. J. Dessler, 1964, Comment on the Paper by Conway W. Snyder et al., "The Solar Wind Velocity and Its Correlation With Cosmic-ray Variations and With Geomagnetic Activity." Journal of Geophysical Research, Vol. 69, 2846.

28. Matsushita, S. (Editor), Physics of Geomagnetic Phenomena. (In Press)

29. McDonald, F. B. (Editor), 1963, Solar Proton Manual, NASA TR R-169.

30. Ness, Norman F., 1966, "Earth's Magnetic Field: A New Look." Science, Vol. 151, 1041-1052.

31. Odishaw, Hugh (Editor) 1966, Research in Geophysics. Cambridge, Massachusetts: The M.I.T. Press.

32. Runcorn, S. K., 1955, "The Earth's Magnetism." Scientific American, Vol. 193, 152-162.

33. Sherry, D. T., 1966, Unpublished Term Paper, University of Michigan.

34. Smith, H. J., and E. V. Smith, 1963, Solar Flares. New York: The MacMillan Co.

35. Snyder, Conway W., Marcia Neugebauer, and U. R. Rao, 1963, "The Solar Wind Velocity and Its Correlation With Cosmic Ray Variations and With Solar and Geomagnetic Activity." Journal of Geophysical Research, Vol. 68, 6361-6370.

36. Solar Forecast Center, 1966, Unpublished Study.

37. Stolov, Harold L., 1965, "Further Investigations of a Variation of Geomagnetic Activity With Lunar Phase." Journal of Geophysical Research, Vol 70, 4921-4926.

38. Swarup, G., 1963, "The Slowly-Varying Component of Solar Radio Emission." AAS-NASA Symposium on the Physics of Solar Flares, 179-197.

39. Tudor, R. F., 1966, Unpublished Study, Solar Forecast Center.

40. United States Air Force, 1965, A Descriptive Summary of the Sun, Solar Phenomena, and Solar-Terrestrial Relationships, 4th Weather Group Phamphlet 105-16-1.

41. Valley, Shea L. (Editor), 1965, Handbook of Geophysics and Space Environments. Air Force Cambridge Research Laboratories: Office of Aerospace Research, USAF.

42. Warwick, C. S., 1963, "Delay Time of PCA and Its Relation to Delay Time of Geomagnetic Disturbance." Journal of Geophysical Research, Vol. 68, 1561-1562.

43. Warwick, C. S., 1965, "Early Recognition of a Solar Flare. II: Energetic Protons." NBS Report 8862.

44. Warwick, C. S., 1965, "Longitude Distribution of Proton Flares." The Astrophysical Journal, Vol. 141, 500-504.

45. Warwick, C. S., 1966, "Sunspot Configurations and Proton Flares." The Astrophysical Journal, Vol. 145, 215-223.

46. Weddell, J. B., and P. J. Leavell, 1963, Long-Range Prediction of Solar Flares from Calcium Plage Measurements. North American Aviation Space and Information Systems Division, SID 63-347.

UNCLASSIFIED

Security Classification

**DOCUMENT CONTROL DATA - R&D**

*(Security classification of title, body of abstract and indexing annotation must be entered when the overall report is classified)*

| | |
|---|---|
| 1. ORIGINATING ACTIVITY *(Corporate author)*<br>Solar Forecast Facility<br>Hq, 4th Weather Wing<br>Ent AFB, Colorado 80912 | 2a. REPORT SECURITY CLASSIFICATION<br>UNCLASSIFIED<br>2b. GROUP |

3. REPORT TITLE

Forecasting Solar Activity and Geophysical Responses

4. DESCRIPTIVE NOTES *(Type of report and inclusive dates)*

n/a

5. AUTHOR(S) *(Last name, first name, initial)*

Staff
Solar Forecast Facility

| 6. REPORT DATE | 7a. TOTAL NO. OF PAGES | 7b. NO. OF REFS |
|---|---|---|
| 30 December 1966 | 57 | 46 |

| | |
|---|---|
| 8a. CONTRACT OR GRANT NO.<br>n/a | 9a. ORIGINATOR'S REPORT NUMBER(S)<br>4WWM 105-1 |
| b. PROJECT NO. | |
| c. | 9b. OTHER REPORT NO(S) *(Any other numbers that may be assigned this report)* |
| d. | |

10. AVAILABILITY/LIMITATION NOTICES

Distribution of this document is unlimited.

| 11. SUPPLEMENTARY NOTES | 12. SPONSORING MILITARY ACTIVITY |
|---|---|
| n/a | n/a |

13. ABSTRACT

This publication presents the philosophy and the techniques involved in producing operational probability forecasts for the occurrence of solar flares and proton events, forecasts of 10-cm solar radio flux, and forecasts of the geomagnetic index $A_p$, and describes the principal parameters and relationships to be considered and evaluated in making these forecasts.

UNCLASSIFIED
Security Classification

| 14. KEY WORDS | LINK A ROLE | LINK A WT | LINK B ROLE | LINK B WT | LINK C ROLE | LINK C WT |
|---|---|---|---|---|---|---|
| Astronomy | | | | | | |
| Astrophysics | | | | | | |
| Geophysics | | | | | | |
| Geomagnetism | | | | | | |
| Solar Flare Prediction | | | | | | |
| Solar Proton Event Prediction | | | | | | |

## INSTRUCTIONS

1. ORIGINATING ACTIVITY: Enter the name and address of the contractor, subcontractor, grantee, Department of Defense activity or other organization *(corporate author)* issuing the report.

2a. REPORT SECURITY CLASSIFICATION: Enter the overall security classification of the report. Indicate whether "Restricted Data" is included. Marking is to be in accordance with appropriate security regulations.

2b. GROUP: Automatic downgrading is specified in DoD Directive 5200.10 and Armed Forces Industrial Manual. Enter the group number. Also, when applicable, show that optional markings have been used for Group 3 and Group 4 as authorized.

3. REPORT TITLE: Enter the complete report title in all capital letters. Titles in all cases should be unclassified. If a meaningful title cannot be selected without classification, show title classification in all capitals in parenthesis immediately following the title.

4. DESCRIPTIVE NOTES: If appropriate, enter the type of report, e.g., interim, progress, summary, annual, or final. Give the inclusive dates when a specific reporting period is covered.

5. AUTHOR(S): Enter the name(s) of author(s) as shown on or in the report. Enter last name, first name, middle initial. If military, show rank and branch of service. The name of the principal author is an absolute minimum requirement.

6. REPORT DATE: Enter the date of the report as day, month, year; or month, year. If more than one date appears on the report, use date of publication.

7a. TOTAL NUMBER OF PAGES: The total page count should follow normal pagination procedures, i.e., enter the number of pages containing information.

7b. NUMBER OF REFERENCES: Enter the total number of references cited in the report.

8a. CONTRACT OR GRANT NUMBER: If appropriate, enter the applicable number of the contract or grant under which the report was written.

8b, 8c, & 8d. PROJECT NUMBER: Enter the appropriate military department identification, such as project number, subproject number, system numbers, task number, etc.

9a. ORIGINATOR'S REPORT NUMBER(S): Enter the official report number by which the document will be identified and controlled by the originating activity. This number must be unique to this report.

9b. OTHER REPORT NUMBER(S): If the report has been assigned any other report numbers *(either by the originator or by the sponsor)*, also enter this number(s).

10. AVAILABILITY/LIMITATION NOTICES: Enter any limitations on further dissemination of the report, other than those imposed by security classification, using standard statements such as:

(1) "Qualified requesters may obtain copies of this report from DDC."

(2) "Foreign announcement and dissemination of this report by DDC is not authorized."

(3) "U. S. Government agencies may obtain copies of this report directly from DDC. Other qualified DDC users shall request through
____________________________________."

(4) "U. S. military agencies may obtain copies of this report directly from DDC. Other qualified users shall request through
____________________________________."

(5) "All distribution of this report is controlled. Qualified DDC users shall request through
____________________________________."

If the report has been furnished to the Office of Technical Services, Department of Commerce, for sale to the public, indicate this fact and enter the price, if known.

11. SUPPLEMENTARY NOTES: Use for additional explanatory notes.

12. SPONSORING MILITARY ACTIVITY: Enter the name of the departmental project office or laboratory sponsoring *(paying for)* the research and development. Include address.

13. ABSTRACT: Enter an abstract giving a brief and factual summary of the document indicative of the report, even though it may also appear elsewhere in the body of the technical report. If additional space is required, a continuation sheet shall be attached.

It is highly desirable that the abstract of classified reports be unclassified. Each paragraph of the abstract shall end with an indication of the military security classification of the information in the paragraph, represented as *(TS)*, *(S)*, *(C)*, or *(U)*.

There is no limitation on the length of the abstract. However, the suggested length is from 150 to 225 words.

14. KEY WORDS: Key words are technically meaningful terms or short phrases that characterize a report and may be used as index entries for cataloging the report. Key words must be selected so that no security classification is required. Identifiers, such as equipment model designation, trade name, military project code name, geographic location, may be used as key words but will be followed by an indication of technical context. The assignment of links, rules, and weights is optional.

UNCLASSIFIED
Security Classification